bioRxiv preprint doi: https://doi.org/10.1101/2019.12.20.885459; this version posted December 21, 2019. The copyright holder for this preprint (which was not certified by peer review) is the author/funder. All rights reserved. No reuse allowed without permission.

1

# Optimal maturation of the SIV-specific CD8$^+$ T-cell response after primary infection is associated with natural control of SIV.

2

3

## ANRS SIC study

4

5 Caroline Passaes[1,2], Antoine Millet[3], Vincent Madelain[4], Valérie Monceaux[1], Annie David[1],
6 Pierre Versmisse[1], Naya Sylla[2], Emma Gostick[5], David A. Price[5], Antoine Blancher[6,7], Nathalie
7 Dereuddre-Bosquet[2], Gianfranco Pancino[1], Roger Le Grand[2], Olivier Lambotte[2,8], Michaela
8 Müller-Trutwin[1], Christine Rouzioux[3,9], Jeremie Guedj[4], Veronique Avettand-Fenoel[3,9], Bruno
9 Vaslin[2#,*], Asier Sáez-Cirión[1#,*]

10

11 [1] Institut Pasteur, HIV Inflammation and Persistence. Paris 75015; France.
12 [2] CEA-Université Paris Sud-INSERM, UMR1184 'Immunology of Viral Infections and Autoimmune Diseases'-
13 IDMIT Department, IBFJ, Fontenay-aux-Roses, France.
14 [3] Université Paris-Descartes, Sorbonne Paris Cité, Faculté de Médecine, EA7327, Paris, France.
15 [4] IAME, UMR 1137, INSERM, Université Paris Diderot, Sorbonne Paris Cité Paris, France.
16 [5] Cardiff University School of Medicine, Division of Infection and Immunity, Cardiff, UK.
17 [6] Laboratoire d'Immunogénétique Moléculaire, EA 3034, Université Paul Sabatier, Toulouse 3, France.
18 [7] Laboratoire d'Immunologie, CHU de Toulouse, Toulouse, France.
19 [8]Assistance Publique-Hôpitaux de Paris, Service de Médecine Interne et Immunologie Clinique, Groupe
20 Hospitalier Universitaire Paris Sud, Hôpital Bicêtre, Le Kremlin-Bicêtre, France
21 [9]Assistance Publique-Hôpitaux de Paris, Service de Microbiologie Clinique, Hôpital Necker-Enfants Malades,
22 Paris, France

23

24 #These authors contributed equally to this work.
25 *Correspondence: asier.saez-cirion@pasteur.fr or bruno.vaslin@cea.fr

26

bioRxiv preprint doi: https://doi.org/10.1101/2019.12.20.885459; this version posted December 21, 2019. The copyright holder for this preprint (which was not certified by peer review) is the author/funder. All rights reserved. No reuse allowed without permission.

27 **ABSTRACT**

28 Highly efficient virus-specific $CD8^+$ T-cells are associated with immune control of HIV
29 infection, but it remains unclear how these cells are generated and maintained over time.
30 We used a macaque model of spontaneous control of SIVmac251 infection to monitor the
31 development and evolution of potent antiviral $CD8^+$ T-cell responses. SIV-specific $CD8^+$ T-
32 cells emerged during primary infection in all animals. However, the ability of $CD8^+$ T cells to
33 suppress SIV replication was low in early stages but increased after a period of maturation,
34 temporally linked with the establishment of sustained low-level viremia in controller
35 macaques. SIV-specific $CD8^+$ T-cells with a central memory phenotype expressed higher
36 levels of survival markers in controllers *versus* non-controllers. In contrast, a persistently
37 skewed differentiation phenotype was observed among central memory SIV-specific $CD8^+$ T-
38 cells in non-controllers since primary infection, typified by relatively high expression levels of
39 T-bet.

40 Collectively, these data show that the phenotype of SIV-specific $CD8^+$ T-cells defined early
41 after SIV infection favor the gain of antiviral potency as a function of time in controllers,
42 whereas SIV-specific $CD8^+$ T-cell responses in non-controllers fail to gain antiviral potency
43 due to early defects imprinted in the central memory pool.

bioRxiv preprint doi: https://doi.org/10.1101/2019.12.20.885459; this version posted December 21, 2019. The copyright holder for this preprint (which was not certified by peer review) is the author/funder. All rights reserved. No reuse allowed without permission.

44 **INTRODUCTION**

45 The ability of CD8+ T-cells to control viral replication has been extensively documented in the
46 setting of HIV/SIV infection (McBrien et al., 2018; Walker and McMichael, 2012). Primary
47 infection is characterized by massive viremia, which subsides following the expansion of
48 HIV/SIV-specific CD8+ T-cells (Borrow et al., 1994; Koup et al., 1994). However, the virus is
49 not eradicated, leading to the emergence of immune escape variants (Allen et al., 2000;
50 Borrow et al., 1997; O'Connor et al., 2002; Price et al., 1997) and to CD8+ T-cell exhaustion
51 during the chronic phase of infection (Day et al., 2006; Petrovas et al., 2006; Petrovas et al.,
52 2007; Trautmann et al., 2006). These observations suggest that naturally generated HIV/SIV-
53 specific CD8+ T-cells are frequently suboptimal in terms of antiviral efficacy, potentially
54 reflecting limited cross-reactivity and/or intrinsic defects in the arsenal of effector functions
55 required to eliminate infected CD4+ T-cells (Du et al., 2016; Lecuroux et al., 2013). The latter
56 possibility is especially intriguing in light of *ex vivo* experiments showing that effective
57 suppression of viral replication is a particular feature of CD8+ T-cells isolated from HIV
58 controllers (HICs) (Angin et al., 2016; Saez-Cirion et al., 2007; Saez-Cirion et al., 2009; Tansiri
59 et al., 2015).

60

61 HICs are a rare group of individuals who control viremia to very low levels without
62 antiretroviral therapy (Saez-Cirion and Pancino, 2013). Understanding the mechanisms
63 associated with such spontaneous control of HIV infection seems crucial for the
64 development of new strategies designed to achieve remission. Efficient CD8+ T-cell
65 responses are almost universally present in HICs (Betts et al., 2006; Chowdhury et al., 2015;
66 Hersperger et al., 2011a; Hersperger et al., 2010; Migueles et al., 2002; Migueles et al., 2008;
67 Saez-Cirion et al., 2007; Saez-Cirion et al., 2009; Zimmerli et al., 2005). These individuals also

bioRxiv preprint doi: https://doi.org/10.1101/2019.12.20.885459; this version posted December 21, 2019. The copyright holder for this preprint (which was not certified by peer review) is the author/funder. All rights reserved. No reuse allowed without permission.

68 frequently express the protective human leukocyte antigen (HLA) allotypes HLA-B*27 and
69 HLA-B*57, further supporting a key role for CD8$^+$ T-cells in the natural control of HIV
70 (Lecuroux et al., 2014; Migueles et al., 2000; Pereyra et al., 2008). However, the presence of
71 protective HLA alleles is neither sufficient nor necessary for natural control of infection, and
72 HICs carrying non-protective HLA class I alleles also carry CD8$^+$ T-cells with strong HIV
73 suppressive capacity (Lecuroux et al., 2014). Although the qualitative properties of CD8$^+$ T-
74 cells from HICs have been extensively characterized, these analyses have been essentially
75 performed during chronic infection, when viremia was already under control, often several
76 years after the acquisition of HIV. It therefore remains unclear how these high-quality CD8$^+$
77 T-cell responses develop from the early stages of infection and evolve over time.
78
79 Cynomolgus macaques (CyMs, *Macaca fascicularis*) infected with SIVmac251 closely
80 recapitulate the dynamics and key features of HIV infection, including similar levels of viral
81 replication in the acute and chronic phases of infection, memory CD4$^+$ T-cell depletion, rapid
82 seeding of the viral reservoir, and eventually progression to AIDS with diarrhea, weight loss,
83 high incidence of lymphoblastic lymphomas and marked decrease of CD4+ T cells within 145
84 to 464 days post-infection (Antony and MacDonald, 2015; Feichtinger et al., 1990; Karlsson
85 et al., 2007; Mannioui et al., 2009; Putkonen et al., 1989). As in humans, some individuals
86 control infection naturally in the absence of treatment. CyMs from Mauritius offer the
87 additional advantage of limited MHC diversity, making them particularly attractive for the
88 study of CD8+ T-cell responses. Indeed, natural SIV control in Mauritius CyMs is favored by
89 the presence of the MHC haplotype M6 (Aarnink et al., 2011; Mee et al., 2009). Natural SIV
90 control can be also achieved in CyMs inoculated with a relatively low virus dose exposure
91 through the intra rectal route (*i.r.*), independent of their MHC haplotype (Bruel et al., 2015).

bioRxiv preprint doi: https://doi.org/10.1101/2019.12.20.885459; this version posted December 21, 2019. The copyright holder for this preprint (which was not certified by peer review) is the author/funder. All rights reserved. No reuse allowed without permission.

92 We therefore took advantage of these validated CyM models spreading from natural SIV
93 control to progression to AIDS to study the dynamics of SIV-specific $CD8^+$ T-cell responses in
94 blood and tissues from the onset of infection in both SIV controllers and viremic macaques.
95 Using this approach, we identified an optimal maturation pathway that enabled SIV-specific
96 $CD8^+$ T-cells to acquire potent antiviral functions, control viremia, and survive in SICs.
97

bioRxiv preprint doi: https://doi.org/10.1101/2019.12.20.885459; this version posted December 21, 2019. The copyright holder for this preprint (which was not certified by peer review) is the author/funder. All rights reserved. No reuse allowed without permission.

98 **RESULTS**

99 ***SIV controllers are characterized by partial restoration of CD4+ T-cell counts and***
100 ***progressive decline in the frequency of SIV-carrying cells in blood***

101 We monitored prospectively the outcome of infection in 12 SIV controllers (SICs) and 4
102 viremic CyMs (VIRs) inoculated *i.r.* with SIVmac251. These animals carried or not the
103 protective M6 haplotype and were inoculated with 5 or 50 animal infectious dose$_{50}$ (AID$_{50}$) of
104 SIVmac251 (Supplemental Table 1). SIV controllers decreased plasma viral load (VL) to levels
105 below 400 SIV-RNA copies/mL, at least twice, over a follow up period of 18 months, while
106 VIRs consistently maintained VL above 400 SIV-RNA copies/mL. The threshold of 400 RNA
107 copies/mL was chosen in coherence with our studies in human cohorts of natural HIV control
108 (Angin et al., 2016; Noel et al., 2016; Saez-Cirion et al., 2013; Saez-Cirion et al., 2007; Saez-
109 Cirion et al., 2009). Ten SICs achieved control of viremia within 3 months. The other two SICs
110 (BL669 and BO413) achieved VL below 400 SIV-RNA copies/mL for the first time 14 months
111 after inoculation. One VIR CyM (AV979) developed a tonsilar lymphoma, an AIDS related
112 event reported at high frequency in this species upon SIV infection (Feichtinger et al., 1990).

113

114 Some differences in peak viremia were observed between SICs and VIRs (Figure 1A, Table 1).
115 These differences became more pronounced over time (Figure 1A), because plasma viremia
116 was suppressed more rapidly in SICs versus VIRs (Table 1). Levels of cell-associated SIV-DNA
117 in blood from SICs and VIRs were comparable before peak viremia, but differences became
118 apparent as plasma VLs declined and were maintained throughout chronic infection (Figure
119 1B, Table 1). In addition, CD4$^{+}$ T-cell counts declined markedly in blood from both SICs and
120 VIRs during primary infection (Figure 1C, Table 1). Subsequently, a degree of recovery was
121 observed in SICs, whereas further gradual decline was observed in VIRs (Figure 1C, Table 1).

bioRxiv preprint doi: https://doi.org/10.1101/2019.12.20.885459; this version posted December 21, 2019. The copyright holder for this preprint (which was not certified by peer review) is the author/funder. All rights reserved. No reuse allowed without permission.

122

123 These results evidenced the distinctive dynamics of SIV infection in SICs and VIRs,
124 characterized by very modest differences during the early weeks following inoculation that
125 were progressively exacerbated during transition to chronic infection. The differences
126 between SICs and VIRs during the chronic phase of SIV infection were consistent with the
127 observations in human cohorts of HIV controllers.

128

129 ***SIV control is associated with early preservation of lymph nodes***

130 To characterize the extent of SIV control in greater depth, we monitored $CD4^+$ T-cells and
131 total SIV-DNA longitudinally in peripheral lymph nodes (PLNs) and rectal biopsies (RBs). At
132 the end of the study, we conducted similar evaluations in bone marrow, spleen, mesenteric
133 lymph nodes (MLNs), and colonic mucosa, comparing SICs versus VIRs. The frequency of
134 $CD4^+$ T-cells similarly declined in RBs from both SICs and VIRs during the acute stage of
135 primary infection. While the frequency of $CD4^+$ T-cells was later partially restored in SICs, it
136 continued to decline in VIRs (Figure 2A). These results matched the observations in blood
137 samples (Figure 1B). In contrast, the frequency of $CD4^+$ T-cells was maintained close to
138 baseline in PLNs from SICs, even during primary infection (day 14 post-infection [*p.i.]*), but
139 steadily declined over time in VIRs (Figure 2B). At the time of euthanasia, $CD4^+$ T-cell
140 frequencies were substantially higher in blood (Figure 1C), bone marrow, spleen, PLNs,
141 MLNs, and colonic mucosa (Figure 2C) from SICs versus VIRs.

142

143 Cell-associated SIV-DNA levels closely mirrored the dynamics of $CD4^+$ T-cells. Similarly high
144 levels of cell-associated SIV-DNA were observed in RBs from SICs and VIRs during primary
145 infection, but lower levels were observed in RBs from SICs *versus* VIRs during chronic

bioRxiv preprint doi: https://doi.org/10.1101/2019.12.20.885459; this version posted December 21, 2019. The copyright holder for this preprint (which was not certified by peer review) is the author/funder. All rights reserved. No reuse allowed without permission.

146 infection (Figure 2D). Of note, SIV-DNA levels were already approximately 1 log lower in
147 PLNs *versus* RBs from SICs during primary infection, and accordingly, lower levels were
148 observed in PLNs from SICs *versus* VIRs since day 14 *p.i.* (Figure 2E). This finding suggests
149 that early viral replication may be contained more efficiently in lymphoid nodes in SICs
150 compared with other explored anatomical compartments. Moreover, SIV-DNA was also
151 detected in alveolar macrophages from all CyMs throughout the course of infection, again at
152 lower levels in SICs *versus* VIRs during chronic infection (Figure S1A, bottom panel). In
153 addition, SIV-DNA levels trended to decline progressively over time in SICs in all tissues
154 analyzed, whereas SIV-DNA levels remained stable after primary infection in VIRs (Figure 1B,
155 2D-F). At the time of euthanasia, SIV-DNA levels were substantially lower in blood (Figure
156 1B), bone marrow, PLNs, MLNs, and gut mucosa (Figure 2F and Figure S1B) from SICs *versus*
157 VIRs.
158
159 Collectively, these data indicate that progressive systemic control of viral replication is
160 achieved in SICs with $CD4^+$ T-cell preservation and lower pan-anatomical reservoirs of SIV-
161 DNA. Our results also underline the early preservation of PLNs in these animals.
162
163 ***The dynamics of $CD8^+$ T-cells expansion and activation do not predict control of SIV***
164 To understand the mechanisms that contribute to immune control of SIV, we first monitored
165 the proliferation and activation dynamics of total $CD8^+$ T-cells in blood and lymphoid tissues
166 from SICs and VIRs. Recent studies in cohorts of hyperacute HIV infected individuals indicate
167 that the changes observed in the total $CD8^+$ T-cell activation during acute infection may be
168 largely related to changes in the HIV-specific $CD8^+$ T-cell pool (Ndhlovu et al., 2015; Takata et
169 al., 2017). The frequencies of $CD8^+$ T-cells expressing Ki-67 in blood increased to maximum

bioRxiv preprint doi: https://doi.org/10.1101/2019.12.20.885459; this version posted December 21, 2019. The copyright holder for this preprint (which was not certified by peer review) is the author/funder. All rights reserved. No reuse allowed without permission.

170 levels during primary infection (measured peak at day 15 *p.i.*), coinciding with the measured
171 peak of viremia, then declined steadily to baseline levels during chronic infection (Figure 3A).
172 Similar dynamics were observed in PLNs (Figure 3B) and gut mucosa (Figure 3C). In general,
173 there were no significant differences between SICs and VIRs with respect to the dynamics of
174 Ki-67 expression within the CD8$^+$ T-cell pool, although lower frequencies of CD8$^+$ T-cells
175 expressing Ki-67 were observed during chronic infection in PLNs from SICs *versus* VIRs
176 (Figure 3B).
177
178 The frequencies of CD8$^+$ T-cells expressing the activation markers CD38 and HLA-DR in blood,
179 PLNs, and gut mucosa increased similarly during primary infection (measured peak at day 28
180 *p.i.*), following the dynamics of Ki-67 expression in the same compartments (Figure 3D–F).
181 Again, there were no significant differences between SICs and VIRs with respect to the early
182 dynamics of total CD8$^+$ T-cell activation, but lower frequencies of CD8$^+$ T-cells expressing
183 CD38 and HLA-DR were observed during chronic infection in PLNs from SICs *versus* VIRs
184 (Figure 3E).
185
186 Overall, our findings indicate that although lower activation and proliferation is observed in
187 of CD8$^+$ T-cells from SICs than VIRs in the chronic stage of infection, the early proliferation
188 and activation dynamics of the total pool of CD8$^+$ T-cells do not distinguish subsequent
189 progression rates.
190
191 ***SIV-specific CD8$^+$ T-cell frequencies do not predict control of SIV***
192 In parallel experiments, we analyzed CD8$^+$ T-cell responses to a pool of optimal SIVmac251
193 peptides, which included peptides from different SIV proteins recognized by the most

bioRxiv preprint doi: https://doi.org/10.1101/2019.12.20.885459; this version posted December 21, 2019. The copyright holder for this preprint (which was not certified by peer review) is the author/funder. All rights reserved. No reuse allowed without permission.

194 frequent MHC haplotypes in CyMs (M1, M2 and M3) and by the MHC haplotype M6
195 (Supplemental Table 2). All the animals carried at least one haplotype matching some
196 peptide, and overall there was not difference in the number of peptides tested theoretically
197 recognized in controllers and non-controllers (p=0.35). SIV-specific CD8$^+$ T-cells producing
198 TNFα (cytokine showing the lowest background in the absence of peptide or in presence of
199 peptide during the baseline and hence used as reference) emerged in all CyMs during
200 primary infection, coinciding with the peak of viremia, and no significant differences were
201 observed between SICs and VIRs with respect to the frequencies of these cells in any
202 anatomical compartment at any stage of infection (Figure 4A). Similarly, no consistent
203 differences were observed between SICs and VIRs with respect to the frequencies of SIV-
204 specific CD8$^+$ T-cells that produced other cytokines, including IFNγ (Figure S2A and S3A) and
205 IL-2 (Figure S2B and S3B), or mobilized CD107a (Figure S2C and S3C). The overall SIV-specific
206 CD8$^+$ T-cell response, determined in each CyM as the frequency of cells displaying at least
207 one function (TNFα, IFNγ, IL-2, or CD107a), was also equivalent between SICs and VIRs
208 across anatomical compartments during primary and chronic infection (Figure S2D and S3D).
209 In addition, no clear differences between SICs and VIRs were observed with respect to the
210 frequencies of SIV-specific CD8$^+$ T-cells displaying at least three functions simultaneously in
211 blood or PLNs during acute infection, but higher frequencies of polyfunctional SIV-specific
212 CD8$^+$ T-cells were present during chronic infection in lymphoid tissues from SICs *versus* VIRs
213 (Figure 4B and S4). Of note, no differences in the magnitude (Figure S5A) and polyfunction
214 (Figure S5B) of SIV-specific CD8$^+$ T-cells from SICs and VIRs were observed either when a pool
215 of overlapping peptides spanning SIV Gag was used instead of the optimal peptide pool to
216 stimulate the cells.
217

bioRxiv preprint doi: https://doi.org/10.1101/2019.12.20.885459; this version posted December 21, 2019. The copyright holder for this preprint (which was not certified by peer review) is the author/funder. All rights reserved. No reuse allowed without permission.

218 These data suggest that natural control of SIV is not associated with acutely generated,
219 functionally superior SIV-specific CD8$^+$ T-cell responses, defined on the basis of cytokine
220 production and degranulation.

221

222 ***Progressive acquisition of CD8$^+$ T-cell-mediated SIV-suppressive activity is associated with***
223 ***control of SIV***

224 CD8$^+$ T-cells from HICs typically suppress *ex vivo* infection of autologous CD4$^+$ T-cells (Angin
225 et al., 2016; Buckheit et al., 2012; Julg et al., 2010; Saez-Cirion et al., 2007; Saez-Cirion et al.,
226 2009; Tansiri et al., 2015). We therefore investigated this property as a potential
227 discriminant between SICs and VIRs. The capacity of CD8$^+$ T-cells in blood and PLNs to
228 suppress infection of autologous CD4$^+$ T-cells was relatively weak in all CyMs during acute
229 infection (Figure 5A), but remarkably, this activity correlated negatively with viremia on day
230 15 *p.i.* (Figure 5B, upper panel) suggesting its contribution to control viremia since early time
231 points. Interestingly, the CD8$^+$ T-cell-mediated SIV-suppressive activity increased
232 substantially over time in SICs (Figure 5A and S6), either in blood or tissues. No such
233 acquisition of SIV-suppressive activity was observed in VIRs (Figure 5A and S6). Moreover,
234 CD8$^+$ T-cell-mediated SIV-suppressive activity on day 70 *p.i.* correlated negatively (or trended
235 to correlate) with all subsequent determinations of plasma VL (Figure S7) and there was a
236 negative correlation between the CD8$^+$ T-cell-mediated SIV-suppressive activity at
237 euthanasia and the viremia at this time (Figure 5C, upper panel). In contrast, no significant
238 correlations were identified at any time point between SIV-specific CD8$^+$ T-cell frequencies,
239 categorized according to TNF$\alpha$ production in response to SIV peptides, and measurements
240 of plasma VL (Figure 5B-C, bottom panels). Moreover, CD8$^+$ T-cell-mediated SIV-suppressive
241 activity across the entire follow-up period, quantified as area under the curve, trended to

bioRxiv preprint doi: https://doi.org/10.1101/2019.12.20.885459; this version posted December 21, 2019. The copyright holder for this preprint (which was not certified by peer review) is the author/funder. All rights reserved. No reuse allowed without permission.

242 correlate negatively with plasma VL ($r_s$ = –0.47, p = 0.07), whereas no such association was
243 identified for the frequency of SIV-specific CD8$^+$ T-cells ($r_s$ = –0.01, p = 0.97) (Figure 5D).
244
245 In a complementary study, Madelain et al (submitted) developed a mathematical model to
246 fit the longitudinal SIV RNA data in this cohort of animals. The best fit to the data was
247 obtained by using a model including an immune-response-mediated infected-cell elimination
248 compartment where the loss rate of productively infected cells increased over time.
249 Interestingly, the pattern of increase in cell loss rates (based on the analysis of SIV RNA only)
250 nicely matched in most animals the changes in the capacity of CD8$^+$ T-cells to suppress
251 infection that were obtained experimentally. Moreover, a *post hoc* positive correlation was
252 found between the theoretical immune-response-mediated infected-cell elimination rate
253 and the experimental CD8$^+$ T-cell-mediated SIV-suppressive activity, but not with the
254 frequency of SIV-specific CD8$^+$ T-cells.
255
256 Therefore, our results exposed a disconnection between the development of SIV-specific
257 CD8$^+$ T-cells producing cytokines and cytolytic molecules and the ability of these cells to
258 suppress SIV infection, as measured *ex vivo* (Figure 5E, Figure S6). SIV-specific CD8$^+$ T-cell
259 frequencies increased sharply as the initial viremia began to fall and remained high for the
260 duration of the study in CyMs irrespectively of their level of viremia. However, the
261 substantial decline in viremia to levels below 400 copies/mL in SICs coincided with the raise
262 of SIV-suppressive activity *ex vivo*. The increase of CD8$^+$ T-cell-mediated SIV-suppressive
263 activity was delayed in the late controller #BL669 and #BO413, but nonetheless preceded
264 optimal control of viremia in these CyMs. A very strong capacity of CD8$^+$ T-cells to suppress
265 SIV was observed at day 36 in the LN from two animals (BA209 and BC657) that did not show

bioRxiv preprint doi: https://doi.org/10.1101/2019.12.20.885459; this version posted December 21, 2019. The copyright holder for this preprint (which was not certified by peer review) is the author/funder. All rights reserved. No reuse allowed without permission.

266 such capacity in the blood (Figure 5A). Only one animal (29925) did not develop any
267 detectable SIV suppressive activity during our follow up. This animal had the weakest peak of
268 viremia (1 log lower than any other) and achieved the fastest control of viremia. Whether a
269 very rapid or local development of the $CD8^+$ T-cell suppressive capacity may have occurred
270 or other mechanisms were associated with control of viremia in this animal remains
271 unknown (Figure S6). At the time of euthanasia, superior $CD8^+$ T-cell-mediated SIV-
272 suppressive activity was detected in a vast majority of SICs across all anatomical
273 compartments, with the exception of bone marrow (Figure 5A), which nonetheless harbored
274 SIV-specific $CD8^+$ T-cells at frequencies comparable to other tissues (Figure 4A). Thus,
275 although abundant, SIV-specific $CD8^+$ T-cells induced during primary SIV infection had limited
276 SIV suppressive capacity when compared to cells found at later time points in SICs (Figure
277 5E).
278
279 To confirm that the capacity of $CD8^+$ T-cells to suppress ex vivo SIV infection did not increase
280 in VIRs, we analyzed this activity in an additional group of 14 non-M6 CyMs infected
281 intravenously (*i.v.*) with 1,000$AID_{50}$ of SIVmac251 and characterized by high setpoint viremia
282 (ANRS pVISCONTI study). In these animals, the $CD8^+$ T-cell-mediated SIV-suppressive activity
283 also remained modest throughout the follow-up (Figure S8A). The combined analysis of the
284 CD8+ T-cells from all VIR CyMs (n=4 50$AID_{50}$ + n=14 1,000$AID_{50}$) exposed early significant
285 differences in the $CD8^+$ T-cell-mediated SIV-suppressive activity when compared to the SICs
286 (Figure S8B). Moreover, early initiation (day 28 post-infection) of antiretroviral treatment in
287 another group of CyM inoculated with 1,000$AID_{50}$ of SIVmac251 sharply decreased viremia
288 and $CD8^+$ T-cell activation levels (Figure S8C) but did not change the capacity of $CD8^+$ T-cells
289 from these animals to suppress infection *ex vivo*, which remained extremely weak (Figure

bioRxiv preprint doi: https://doi.org/10.1101/2019.12.20.885459; this version posted December 21, 2019. The copyright holder for this preprint (which was not certified by peer review) is the author/funder. All rights reserved. No reuse allowed without permission.

290 S8C). These results, which are in agreement with our previous observations in early treated
291 HIV-infected individuals (Lecuroux et al., 2013), show that low SIV suppressive capacity
292 during acute infection was neither a consequence of strong activation of these cells *in vivo*
293 nor of high antigen burden.
294
295 Collectively, our results show that the capacity of SIV-specific CD8$^+$ T-cells to suppress
296 infection *ex vivo* was a genuine quality that progressively amplifies in SICs. Our results
297 further uncover a temporal link between the acquisition by CD8$^+$ T-cells of potent capacity to
298 suppress infection and sustained control of SIV.
299
300 ***Acquisition of CD8$^+$ T-cell-mediated SIV-suppressive activity in SICs occurs independently of***
301 ***MHC haplotype***
302 Our primary intention in this study was to explore the mechanisms underlying natural
303 control of SIV infection, independently of MHC background or infectious dose. However, as
304 expected (Bruel et al., 2015), inoculation with low-dose virus and carriage of the protective
305 M6 haplotype independently favored spontaneous control of viremia below 400 copies/mL
306 in CyMs in our study (Supplemental Table 3). We therefore evaluated whether these
307 parameters influenced the dynamics of control and the development of the CD8$^+$ T-cell
308 response upon infection. We found that CD4$^+$ T-cells and the levels of cell-associated SIV
309 DNA similarly evolved in the blood and PLNs from M6 and non-M6 controllers (Figure S9A).
310 There was just a tendency for M6 controllers vs non-M6 controllers to better recovery of
311 CD4$^+$ T-cells in blood at the end of the study (p=0.07). Similarly, we did not find important
312 differences between M6 and non-M6 controllers in their development of SIV-specific CD8$^+$ T-
313 cell responses (Figure S9B). M6 and non-M6 controllers developed similar frequencies of SIV-

bioRxiv preprint doi: https://doi.org/10.1101/2019.12.20.885459; this version posted December 21, 2019. The copyright holder for this preprint (which was not certified by peer review) is the author/funder. All rights reserved. No reuse allowed without permission.

314 responding cells during acute infection that were maintained during the follow up. Of note,
315 the capacity of CD8$^+$ T-cells to suppress *ex vivo* SIV infection of CD4$^+$ T-cells progressively
316 increased in both M6 and non-M6 controllers. The only difference that we could appreciate
317 was a faster acquisition (day 36 *p.i.*) of CD8$^+$ T-cell mediated SIV suppressive activity in the
318 PLN from M6 SICs versus non-M6 SICs (Figure S9B). Intriguingly, non-M6 SICs had higher
319 frequencies of SIV responding CD8$^+$ T-cells in this tissue at the same time point. Overall these
320 results show that while the M6 background gave a selective advantage to CyMs to control
321 infection in conditions of higher viral inoculum, this MHC haplotype was not indispensable
322 for the acquisition of SIV suppressive capacity by CD8$^+$ T-cells, which occurred both in M6
323 and non M6 SICs. The results are in agreement with the observations in HIV controllers.
324 Although cohorts of HICs are enriched in individuals carrying protective HLA class I alleles
325 (mainly HLA-B*57, B*27), many HICs do not carry protective HLA class I alleles but have CD8$^+$
326 T-cells with strong HIV suppressive capacity *ex vivo* (Lecuroux et al., 2014). Therefore, the
327 development of efficient CD8$^+$ T-cell responses with antiviral activity is a characteristic of
328 most HICs/SICs, independently of their MHC background.
329

330 ***Skewed maturation of central memory SIV-specific CD8$^+$ T-cells is associated with defective***
331 ***acquisition of SIV-suppressive activity***

332 To dissect the phenotypic correlates of *ex vivo* measured antiviral potency, we analyzed the
333 differentiation status of SIV-specific CD8$^+$ T-cells using selected markers in conjunction with
334 MHC class I tetramers (Figure S10, S11). Tetramer-binding SIV-specific CD8$^+$ T-cells were
335 detected in all CyMs, displayed early similar differentiation profiles in SICs and VIRs, but
336 evolved differently, such that higher frequencies of central memory (CM) SIV-specific CD8$^+$ T-

bioRxiv preprint doi: https://doi.org/10.1101/2019.12.20.885459; this version posted December 21, 2019. The copyright holder for this preprint (which was not certified by peer review) is the author/funder. All rights reserved. No reuse allowed without permission.

337 cells were present in SICs versus VIRs on day 105 *p.i.* (p = 0.018) and day 535 *p.i.* (p = 0.013)
338 (Figure 6A, B).
339
340 In further analyses, we found that higher frequencies of SIV-specific CD8$^+$ T-cells from SICs
341 expressed the IL-7 receptor CD127, which is associated with cell survival and memory
342 responses (Schluns et al., 2000), whereas higher frequencies of SIV-specific CD8$^+$ T-cells from
343 VIRs expressed the transcription factor T-bet, which is associated with cellular differentiation
344 and effector functionality (Sullivan et al., 2003; Szabo et al., 2002) (Figure 7A). These
345 differences appeared since primary infection and became statistically significant at later time
346 points (Figure 7A). Expression levels of CD127 and T-bet also varied as a function of
347 differentiation among SIV-specific CD8$^+$ T-cells from SICs and VIRs (Figure 7B). In particular,
348 CM and transitional memory (TM) SIV-specific CD8$^+$ T-cells expressed lower levels of T-bet
349 throughout the course of infection in SICs *versus* VIRs, whereas CM SIV-specific CD8$^+$ T-cells
350 tended to express higher levels of CD127 during chronic infection in SICs *versus* VIRs.
351
352 Accordingly, negative correlations were observed during primary infection and at euthanasia
353 between the expression levels of CD127 on SIV-specific CD8$^+$ T cells and plasma viral loads
354 (Figure 8A). Of note, the levels of CD127 correlated positively with CD8$^+$ T-cell-mediated SIV-
355 suppressive activity at the same time points (Figure 8B). On the contrary, negative
356 correlations were observed during primary infection and at euthanasia between CD8$^+$ T-cell-
357 mediated SIV-suppressive activity and the contemporaneous frequencies of T-bet$^+$CD127$^-$
358 SIV-specific CD8$^+$ T-cells (Figure 8C) and between CD8$^+$ T-cell-mediated SIV-suppressive
359 activity and expression levels of T-bet among CM SIV-specific CD8$^+$ T-cells (Figure 8D).
360

bioRxiv preprint doi: https://doi.org/10.1101/2019.12.20.885459; this version posted December 21, 2019. The copyright holder for this preprint (which was not certified by peer review) is the author/funder. All rights reserved. No reuse allowed without permission.

361 Collectively, these results suggest that SIV-specific CM CD8$^+$ T-cells are primed for survival in
362 SICs, enabling long-term memory, sustained antiviral activity and viral control, whereas the
363 corresponding SIV-specific CD8$^+$ T-cells in VIRs adopt a skewed phenotype associated with
364 cellular differentiation and suboptimal antiviral activity.

bioRxiv preprint doi: https://doi.org/10.1101/2019.12.20.885459; this version posted December 21, 2019. The copyright holder for this preprint (which was not certified by peer review) is the author/funder. All rights reserved. No reuse allowed without permission.

365 **DISCUSSION**

366 The data presented in this study provide new insights into the immune correlates of natural
367 control of SIV. Although SIV-specific $CD8^+$ T-cells were generated during acute infection with
368 equivalent dynamics and global frequencies in all CyMs, preventing discrimination between
369 SICs and VIRs, antiviral efficacy *ex vivo* developed progressively over time and was associated
370 with spontaneous SIV control. This dichotomy was underpinned by distinct early memory
371 programs within the SIV-specific $CD8^+$ T-cell pool. Collectively, these findings identify a
372 cohesive set of immunological parameters that associate with effective and sustained
373 control of SIV.

374

375 To monitor the establishment of natural control prospectively, we took advantage of
376 previous reports showing that carriage of the MHC haplotype M6 and *i.r.* inoculation with
377 low-dose (5AID$_{50}$) virus independently favor spontaneous control of SIVmac251 infection in
378 CyMs (Aarnink et al., 2011; Bruel et al., 2015; Mee et al., 2009). Our results corroborate
379 previous reports. In particular, although the presence M6 haplotype favored more frequent
380 and more rapid control of infection among animals receiving a high dose of the virus
381 (50AID$_{50}$) (Supplemental Table 3), no significant differences were observed in the dynamics
382 of SIV control in M6 and non-M6 controllers. At the time of euthanasia, a higher proportion
383 of $CD4^+$ T-cells and lower cell-associated SIV-DNA levels were found in multiple tissues from
384 SICs *versus* VIRs, demonstrating systemic control of SIV. These differences were much more
385 subtle during primary infection. However, PLNs from SICs harbored approximately 10-fold
386 less SIV-DNA in the acute phase than PLNs from VIRs. In addition, the frequency of $CD4^+$ T-
387 cells were maintained close to baseline throughout the course of the study in PLNs, but not
388 in blood or RBs, from SICs. These observations suggest that early containment of viral

bioRxiv preprint doi: https://doi.org/10.1101/2019.12.20.885459; this version posted December 21, 2019. The copyright holder for this preprint (which was not certified by peer review) is the author/funder. All rights reserved. No reuse allowed without permission.

389 replication in lymph nodes (Buggert et al., 2018; Reuter et al., 2017) may be a key event for
390 subsequent immune control of SIV.
391
392 In line with previous studies in humans (Lecuroux et al., 2013; Ndhlovu et al., 2015;
393 Trautmann et al., 2012) and non-human primates we observed early and robust expansions
394 of SIV-specific CD8$^+$ T-cells in all CyMs. However, the functional profiles and overall
395 frequencies of SIV-specific CD8$^+$ T-cells (as determined by intra cellular cytokine staining
396 upon SIV antigen stimulation) during the acute phase of infection were largely equivalent in
397 SICs and VIRs, and neither parameter correlated with subsequent determinations of plasma
398 VL. Similarly, the functional profiles and overall frequencies of SIV-specific CD8$^+$ T-cells
399 during the chronic phase of infection were largely equivalent in SICs and VIRs, although
400 polyfunctionality (defined as the capacity to produce simultaneously several cytokine and/or
401 degranulate) was impaired at the time of euthanasia in VIRs. These results suggest that
402 differences in polyfunctionality found during chronic infection are a surrogate marker of viral
403 replication rather than an accurate determinant of antiviral efficacy, although low number of
404 animals in the VIR group may limit statistical power.
405
406 The capacity of CD8$^+$ T-cells to suppress infection of autologous CD4$^+$ T-cells directly *ex vivo*
407 is a particular feature of HICs (Almeida et al., 2009; Angin et al., 2016; Buckheit et al., 2012;
408 Julg et al., 2010; Saez-Cirion et al., 2007; Saez-Cirion et al., 2009; Tansiri et al., 2015) that is
409 mediated by the rapid elimination of infected CD4+ T-cells (Saez-Cirion et al., 2007).
410 Irrespective of subsequent outcome, we detected relatively weak CD8$^+$ T-cell-mediated SIV-
411 suppressive activity during primary infection, despite the vigorous mobilization of SIV-
412 specific CD8$^+$ T-cells. This observation parallels our previous findings in the setting of HIV

bioRxiv preprint doi: https://doi.org/10.1101/2019.12.20.885459; this version posted December 21, 2019. The copyright holder for this preprint (which was not certified by peer review) is the author/funder. All rights reserved. No reuse allowed without permission.

413 (Lecuroux et al., 2013) and point to limited antiviral potential of CD8$^+$ T-cell responses
414 generated during primary infection. However, a remarkable negative correlation was already
415 observed between the CD8$^+$ T-cell-mediated SIV-suppressive activity and viremia at this early
416 time point, showing early temporal association of this antiviral activity and reduction of
417 viremia. Of note, this SIV-suppressive capacity of CD8$^+$ T-cells increased progressively over a
418 period of weeks in some animals, carrying or not the protective MHC haplotype M6, and
419 correlated temporally with the establishment of viral control. At the time of euthanasia,
420 these highly potent antiviral CD8$^+$ T-cells were present in all tissues, with the exception of
421 bone marrow. It is important to notice that CD8$^+$ T-cell-mediated SIV suppression was very
422 weak also in LN during the first weeks following infection but increased over time in SICs.
423 Therefore, the increase in the capacity of CD8$^+$ T-cells to suppress infection that we observed
424 in this study was not the result of the recirculation of CD8$^+$ T-cells from lymph nodes once
425 control was established but a genuine progressive augmentation of the antiviral potential of
426 the cells. The development of potent antiviral CD8$^+$ T-cells is therefore a *bone fide* correlate
427 of sustained control of SIV.
428
429 The divergent antiviral properties of SIV-specific CD8$^+$ T-cells in SICs *versus* VIRs were
430 associated with early differences in the expression of CD127 and T-bet, especially within the
431 less differentiated memory pools (CM and TM). In particular, higher frequencies of SIV-
432 specific CM CD8$^+$ T-cells expressed CD127 in SICs, whereas higher frequencies of SIV-specific
433 CM and TM CD8$^+$ T-cells expressed T-bet in VIRs. These differences became more
434 pronounced throughout the course of infection. Studies in mice have shown that decreased
435 expression of T-bet among memory CD8$^+$ T-cells allows the establishment of long-lived
436 CD127$^{hi}$ cells, which maintain the capacity to proliferate and control successive infections

bioRxiv preprint doi: https://doi.org/10.1101/2019.12.20.885459; this version posted December 21, 2019. The copyright holder for this preprint (which was not certified by peer review) is the author/funder. All rights reserved. No reuse allowed without permission.

437 (Joshi et al., 2007; Joshi et al., 2011). Accordingly, our data suggest that SICs develop true
438 memory-like SIV-specific CD8$^+$ T-cell responses, which is key for the acquisition of antiviral
439 ability, whereas VIRs develop SIV-specific memory CD8$^+$ T-cell responses skewed towards
440 more effector-like characteristics. In line with this supposition, the proportion of CD127$^+$ SIV-
441 specific CD8$^+$ T cells during acute infection (day 15 *p.i.*) and at euthanasia correlated
442 positively with CD8$^+$ T-cell-mediated SIV-suppressive activity at the corresponding time
443 points, while the frequencies of T-bet$^+$ CD127$^-$ SIV-specific CD8$^+$ T-cells and the expression
444 levels of T-bet among CM SIV-specific CD8$^+$ T-cells during acute infection correlated
445 negatively with CD8$^+$ T-cell-mediated SIV-suppressive activity. These findings are broadly
446 consistent with several previous reports describing immune profiles that associate with the
447 control of viremia in HICs during chronic infection. Favorable characteristics include high
448 frequencies of CD57$^+$ eomesodermin$^{hi}$ HIV-specific CD8$^+$ T-cells with superior proliferative
449 capacity, increased expression levels of CD127, and intermediate expression levels of T-bet
450 (Simonetta et al., 2014), and high frequencies of HIV-specific CD8$^+$ T-cells with the capacity
451 to upregulate T-bet, granzyme B, and perforin in response to antigen encounter (Hersperger
452 et al., 2011b; Migueles et al., 2008).
453
454 In a recent single cell study (Angin et al., 2019b), we also found differences in the program of
455 HIV-specific CM CD8$^+$ T-cells from HIV controllers and non-controllers on cART: whereas HIV-
456 specific CM CD8$^+$ T-cells from HIC upregulated the expression of effectors genes linked with
457 mTORC2 activation and cell survival (including CD127), central memory cells from non-
458 controllers had a skewed profile associated with mTORC1 activation (including T-bet) and
459 glycolysis. This was traduced in a dependency on glucose of HIV-specific CD8+ T-cells from
460 non-controllers to react to HIV antigens, while HIV-specific CD8+ T-cells from controllers

bioRxiv preprint doi: https://doi.org/10.1101/2019.12.20.885459; this version posted December 21, 2019. The copyright holder for this preprint (which was not certified by peer review) is the author/funder. All rights reserved. No reuse allowed without permission.

461 were characterized by metabolic plasticity and being able to exert their function even in
462 conditions of glucose deprivation. Of note, these differences in the metabolic program of
463 cells from controllers and non-controllers could also be recapitulated with SIV-specific CD8+
464 T-cells from SICs and VIR CyMs from the present study (Angin et al., 2019b), further
465 corroborating the validity of our CyM model to study the development of the protective
466 CD8+ T-cell responses characteristics of HIV/SIV controllers. The present results extend these
467 observations and support a key role for long-lived memory responses in the control of SIV.
468 Importantly, our data also show that distinct memory responses are formed early after
469 infection, potentially reflecting different priming conditions. Interestingly, although the
470 antiviral activity of $CD8^+$ T-cells increased over time in SICs, we already found a negative
471 correlation between this activity and the plasma viremia at day 15. On this basis, we propose
472 that the amplification of potent antiviral activity maters in long term control and is the result
473 of a maturation process, the trajectory of which is linked to early optimal programming of
474 the $CD8^+$ T-cell memory compartment.
475
476 It remains unclear which factors are required to encourage the development of memory
477 $CD8^+$ T-cell responses that provide optimal protection against HIV/SIV. In some viral
478 infections, expression of T-bet is tightly regulated by cytokines, such as IL-12 (Rao et al.,
479 2012; Takemoto et al., 2006). Low levels of inflammation may therefore favor the
480 emergence of long-lived memory $CD8^+$ T-cells. It is also interesting to note that maturation
481 through persistent or repeated exposure to antigen can drive the selection of specific
482 clonotypes bearing high-affinity T-cell receptors (TCRs) (Busch and Pamer, 1999; Ozga et al.,
483 2016; Price et al., 2005) which have been shown to suppress HIV replication more efficiently
484 than clonotypes targeting the same antigen via low-affinity TCRs (Almeida et al., 2007;

bioRxiv preprint doi: https://doi.org/10.1101/2019.12.20.885459; this version posted December 21, 2019. The copyright holder for this preprint (which was not certified by peer review) is the author/funder. All rights reserved. No reuse allowed without permission.

485 Almeida et al., 2009; Ladell et al., 2013). Increase in antigen sensitivity over time would be
486 compatible with the progressive increase in antiviral potency that we observed for the $CD8^+$
487 T-cells from controllers in our study.
488
489 A recent study in the LCMV murine model of infection has shown that memory $CD8^+$ T-cell
490 responses expressing the transcription factor TCF1 developed during chronic infection (in an
491 immunosuppressive environment) have a distinct molecular program, resist contraction, had
492 increased long-term functionality, are less prone to exhaustion and are thus critical for
493 controlling ongoing viral replication; in contrast, memory cells that are developed at the
494 onset of infection (in a pro-inflammatory environment) become short-term effectors and are
495 rapidly exhausted (Snell et al., 2018). Accordingly, we suggest that balanced inflammatory
496 responses (Barouch et al., 2016) arising as a consequence of lower viral burdens in lymph
497 nodes during acute infection in SICs might facilitate antigen-specific priming events
498 associated with optimal memory programs (Ozga et al., 2016) and minimize the loss of $CD4^+$
499 T-cells, which provide helper functions that are critical for the development of long-lived
500 memory $CD8^+$ T-cells (Khanolkar et al., 2004).
501
502 Collectively, the data presented here underscore the importance of early host-pathogen
503 interactions in the development of adaptive immunity and reveal an optimal maturation
504 pathway associated with the generation and maintenance of potent and sustained antiviral
505 $CD8^+$ T-cell responses, which in turn dictate the outcome of infection with SIV.

bioRxiv preprint doi: https://doi.org/10.1101/2019.12.20.885459; this version posted December 21, 2019. The copyright holder for this preprint (which was not certified by peer review) is the author/funder. All rights reserved. No reuse allowed without permission.

506 **METHODS**

507 ***Ethical statement***

508 Cynomolgus macaques (CyMs, *Macaca fascicularis*) were imported from Mauritius and
509 housed in facilities at the *Commissariat à l'Energie Atomique et aux Energies Alternatives*
510 (CEA, Fontenay-aux-Roses, France). All non-human primate studies at the CEA are conducted
511 in accordance with French National Regulations under the supervision of National Veterinary
512 Inspectors (CEA Permit Number A 92-03-02). The CEA complies with the Standards for
513 Human Care and Use of Laboratory Animals of the Office for Laboratory Animal Welfare
514 under Assurance Number #A5826-01. All experimental procedures were conducted
515 according to European Directive 2010/63 (Recommendation Number 9). The SIC and
516 pVISCONTI studies were approved and accredited under statement number A13-005 and
517 A15-035 by the ethics committee *"Comité d'Ethique en Expérimentation Animale du CEA"*,
518 registered and authorized under Number 44 and Number 2453-2015102713323361v2 by the
519 French Ministry of Education and Research. CyMs were studied with veterinary guidance,
520 housed in adjoining individual cages allowing social interactions, and maintained under
521 controlled conditions with respect to humidity, temperature, and light (12 hour light/12
522 hour dark cycles). Water was available *ad libitum*. Animals were monitored and fed once or
523 twice daily commercial monkey chow and fruit by trained personnel. Environmental
524 enrichment was provided including toys, novel foodstuffs, and music under the supervision
525 of the CEA Animal Welfare Body. Experimental procedures (animal handling, viral
526 inoculations, and samplings) were conducted after sedation with ketamine chorhydrate
527 (Rhone-Merieux, Lyon, France, 10 mg/kg). Tissues were collected at necropsy: animals were
528 sedated with ketamine chlorhydrate 10 mg/kg) then humanely euthanized by intravenous
529 injection of 180 mg/kg sodium pentobarbital.

bioRxiv preprint doi: https://doi.org/10.1101/2019.12.20.885459; this version posted December 21, 2019. The copyright holder for this preprint (which was not certified by peer review) is the author/funder. All rights reserved. No reuse allowed without permission.

530

531 ***Animals and SIV infection***

532 A total of 16 healthy adult male CyMs (median age = 6.8 years at inclusion, IQR = 5.8–7.2)
533 were selected for this study on the basis of MHC haplotype ($M6^+$, n = 6; $M6^–$, n = 10) *(34)*.
534 CyMs were inoculated *i.r.* with either $5AID_{50}$ or $50AID_{50}$ of uncloned SIVmac251 (A.M.
535 Aubertin, Université Louis Pasteur, Strasbourg, France). The following experimental groups
536 were studied: (i) $M6^–$ CyMs inoculated *i.r.* with $5AID_{50}$ (non-M6 $5AID_{50}$, n = 4); (ii) $M6^+$ CyMs
537 inoculated *i.r.* with $50AID_{50}$ (M6 $50AID_{50}$, n = 6); and (iii) $M6^–$ CyMs inoculated *i.r.* with
538 $50AID_{50}$ (non-M6 $50AID_{50}$, n = 6). Animals were monitored for 18 months post-infection.

539

540 The outcome of infection generally matched expectations based on previous studies for each
541 experimental group (Figure S12, Supplemental Table 1). Only one $M6^+$ CyM (31041) was
542 unable to control viremia below 400 copies/mL. This animal was homozygous for MHC class I
543 (Supplemental Table 1), which intrinsically limits immune control of HIV/SIV (Carrington et
544 al., 1999; O'Connor et al., 2010). The dynamics of viral replication during acute infection
545 were very similar in the three experimental groups, with peak VLs of 5.9, 6.4, and 6.3 log SIV-
546 RNA copies/mL of plasma on day 14 *p.i.* for non-M6 $5AID_{50}$, M6 $50AID_{50}$, and non-M6
547 $50AID_{50}$ CyMs, respectively (Supplemental Table 1).

548

549 CyMs in the pVISCONTI study (median age = 5 years at inclusion, IQR = 4.1–5.3) were
550 inoculated with 1000 $AID_{50}$ of uncloned SIVmac251 through the intravenous route. None of
551 these animals carried the M6 haplotype. An antiretroviral regimen containing emtricitabine
552 (FTC), dolutegravir (DTG), and the tenofovir prodrug tenofovir-disoproxil-fumarate (TDF), co-

bioRxiv preprint doi: https://doi.org/10.1101/2019.12.20.885459; this version posted December 21, 2019. The copyright holder for this preprint (which was not certified by peer review) is the author/funder. All rights reserved. No reuse allowed without permission.

553 formulated as a once daily subcutaneous injection, was initiated at day 28 post-inoculation
554 in 6 animals. TDF was administered at 5.1 mg/kg, FTC at 40 mg/kg and DTG at 2.5 mg/kg.
555

556 ***Blood collection and processing***

557 Peripheral blood was collected by venous puncture into Vacutainer Plus Plastic K3EDTA
558 Tubes or Vacutainer CPT Mononuclear Cell Preparation Tubes with Sodium Heparin (BD
559 Biosciences). Complete blood counts were monitored at all time points from the Vacutainer
560 Plus Plastic K3EDTA Tubes. Plasma was isolated from Vacutainer Plus Plastic K3EDTA Tubes
561 by centrifugation for 10 min at 1,500 g and stored at –80 °C. Peripheral blood mononuclear
562 cells (PBMCs) were isolated from Vacutainer CPT Mononuclear Cell Preparation Tubes with
563 Sodium Heparin according to manufacturer's instructions (BD Biosciences), and red blood
564 cells were lysed in ACK ($NH_4Cl$ 0.15 M, $KHCO_3$ 10 mM, EDTA 0.1 mM, pH 7.4).
565

566 ***Tissue collection and processing***

567 Axillary or inguinal lymph nodes (PLNs), rectal biopsies (RBs) and broncho-alveolar lavages
568 (BAL) were collected longitudinally from each animal at the indicated time points. In
569 addition, bone marrow, spleen, mesenteric lymph nodes (MLNs), duodenum, jejunum, ileum
570 and colon were collected at necropsy. Tissue samples were snap-frozen in liquid nitrogen for
571 storage at –80 °C or collected in RPMI medium at 2–8 °C. At each time point a complete PLN
572 group was collected. LNs were washed and cells were freshly isolated in RPMI medium upon
573 mechanical disruption with a GentleMACS dissociator as recommended by the manufacturer
574 (Miltenyi Biotec). Cell suspension was filtered (70µm), then red blood cells were lysed in
575 ACK. RB lymphocytes were obtained from approximately 4 $mm^2$ of rectal mucosa. Colonic
576 lymphocytes were obtained from mucosa taken from approximately 10 cm of tissue. RBs and

bioRxiv preprint doi: https://doi.org/10.1101/2019.12.20.885459; this version posted December 21, 2019. The copyright holder for this preprint (which was not certified by peer review) is the author/funder. All rights reserved. No reuse allowed without permission.

577 colonic tissue were washed extensively in R10 medium (RPMI medium supplemented with
578 10% fetal calf serum and penicillin/neomycin/streptomycin), then digested for 45 minutes
579 with collagenase II prior to mechanical disruption. Lymphocytes were isolated over a Percoll
580 67/44 gradient (Sigma-Aldrich). Bone marrow cells were purified using Lymphocyte
581 Separation Medium (Lonza Bioscience) diluted to 90% in DPBS, centrifuged for 20 minutes at
582 350 g, and separated from red cells in ACK. Spleen cells were processed by mechanical
583 disruption in RPMI medium using a GentleMACS™ Dissociator (Miltenyi Biotec), purified as
584 described for bone marrow cells, and separated from red cells in ACK. Total cells were
585 immediately designated to T-cell activation and proliferation analyses by flow cytometry,
586 $CD4^+$ and $CD8^+$ T-cells separation with magnetic beads for antiviral activity assay and the
587 remaining cells were frozen for further assessment of cytokine production by ICS or tetramer
588 analyses.
589

590 ***Quantification of plasma viral load***

591 Plasma viremia was monitored longitudinally in all animals using quantitative real-time
592 RTqPCR with a limit of detection of 12.3 copies/mL (Angin et al., 2019a). Viral RNA was
593 prepared from 100 µl of cell-free plasma. Quantitative RT-PCR was performed with a
594 SuperScript III Platinum One-Step qRT-PCR Kit (Thermofisher) in a CFX96 Touch Real-Time
595 PCR Detection System (BioRad) under the following conditions: 12.5 µl of 2X reaction
596 mixture, 0.5 µl of RNaseOUT (40U/µl), 0.5 µl of Superscript III reverse transcriptase/Platinum
597 Taq DNA Polymerase, 1 µl of each primer (125 µM), 0.5 µl of the fluorogenic probe (135 µM),
598 and 10-µl of RNA elution samples. The probe and primers were designed to amplify a region
599 of SIVmac251 *gag*. Forward primer was 5'-GCAGAGGAGGAAATTACCCAGTAC-3' (24 bp) and
600 reverse primer was 5'-CAATTTTACCCAGGCATTTAATGTT-3' (25 bp). The TaqMan probe

bioRxiv preprint doi: https://doi.org/10.1101/2019.12.20.885459; this version posted December 21, 2019. The copyright holder for this preprint (which was not certified by peer review) is the author/funder. All rights reserved. No reuse allowed without permission.

601 sequence was 5'-FAM-TGTCCACCTGCCATTAAGCCCGA-BHQ1-3' (23 bp). This probe had a
602 fluorescent reporter dye, FAM (6-carboxyfluorescein), attached to its 5' end and the
603 quencher BHQ1 (Black Hole Quencher 1) attached to its 3' end. Samples were heated for 30
604 min at 56°C and 5 min at 95°C, followed by 50 cycles of 95°C for 15 s and 60°C for 1 min.
605

606 ***Quantification of SIV-DNA***

607 Total DNA was extracted from purified $CD14^+$ alveolar macrophages, buffy coats and snap-
608 frozen tissues. $CD14^+$ alveolar macrophages were purified by positive selection using
609 antibody-coated magnetic beads following manufacturer`s instructions (Miltenyi Biotec).
610 Purity was checked by flow cytometry (Figure S1A, upper panel). Snap-frozen tissues were
611 mechanically disrupted with a MagNA Lyser (Roche Diagnostics). DNA extraction was
612 performed using a QIAamp DNA Blood Mini Kit (Qiagen) following manufacturer`s
613 instructions. SIV-DNA was quantified using an ultrasensitive quantitative real-time PCR. For
614 blood samples, 150,000 cells were analyzed for each SIV-DNA PCR. Due to sample size
615 limitations, for rectal biopsies and bronchoalveolar lavages 50,000 and 20,000 cells per PCR
616 were tested, respectively. All amplifications were performed on 2–4 replicates. The cell line
617 SIV1C, which contains 1 copy of SIV integrated/cell, was used as a standard for
618 quantification. 1 µg of DNA was considered to be equivalent to 150,000 cells. Amplification
619 was performed using primers and a probe located in the *gag* region. The *CCR5* gene was
620 used to normalize results per million cells. Results were then adjusted by the frequencies of
621 $CD4^+$ T-cells in blood and tissues, when available. The limit of quantification was 2
622 copies/PCR. Primers and probes were: SIV *gag* F: 5'-GCAGAGGAGGAAATTACCCAGTAC-3'; SIV
623 *gag* R: 5'-CAATTTTACCCAGGCATTTAATGTT-3'; SIV *gag* probe: 5'-FAM-
624 TGTCCACCTGCCATTAAGCCCGA-BHQ1-3'; *CCR5* F: an equimolar mix of 5'-

bioRxiv preprint doi: https://doi.org/10.1101/2019.12.20.885459; this version posted December 21, 2019. The copyright holder for this preprint (which was not certified by peer review) is the author/funder. All rights reserved. No reuse allowed without permission.

625 CAACATGCTGGTCgATCCTCAT-3' and 5'-CAACATACTGGTCGTCCTCATCC-3'; *CCR5* R: 5'-
626 CAGCATAGTGAGCCCAGAAG-3'; and *CCR5* probe: 5'-HEX-CTGACATCTACCTGCTCAACCTG-
627 BHQ1-3'.
628
629 ***Measurement of T-cell activation and proliferation***
630 T-cell activation and proliferation were assessed using fresh PBMCs and tissue cell
631 suspensions. Blood samples were treated with FACS Lysing Solution (BD Biosciences). Cells
632 were surface stained for CD3, CD4, CD8, CD38, CD45, CCR5, and HLA-DR,
633 fixed/permeabilized using a Cytofix/CytoPerm Kit (BD Biosciences), and stained
634 intracellularly for Ki-67. The following antibodies used were: anti-CD3–PE (clone SP34-2, BD
635 Biosciences), anti-CD4–PerCP-Cy5.5 (clone L200, BD Biosciences), anti-CD8–BV650 (clone
636 RPA-T8, BioLegend), anti-CD38–FITC (clone AT-1, StemCell Technologies), anti-CD45–V500
637 (clone D058-1283, BD Biosciences), anti-CCR5–APC (clone 3A9, BD Biosciences), anti-HLA-
638 DR–APC-H7 (clone G46-6, BD Biosciences), and anti-Ki-67–AF700 (clone B56, BD
639 Biosciences). Data were acquired using an LSRII flow cytometer (BD Biosciences) and
640 analyzed with FlowJo software version 10 (TreeStar Inc.).
641
642 ***Intracellular cytokine staining***
643 Frozen PBMCs, PLN cells, bone marrow cells, splenocytes and MLN cells were thawed,
644 resuspended at $1 \times 10^6$/mL in R20 medium, and stored overnight at 37 °C. Cells were then
645 stimulated with a pool of 24 optimal SIV peptides (8-10 amino acids long) (2 µg/mL each,
646 Supplemental Table 2) or with a pool of 125 overlapping SIV Gag 15-mer peptides (2 µg/mL
647 each, NIH AIDS Reagent Program, SIVmac239 Gag Peptide Set #12364) in the presence of
648 anti-CD28 (1 µg/mL, clone L293, BD Biosciences) and anti-CD49d (1 µg/mL, clone 9F10, BD

bioRxiv preprint doi: https://doi.org/10.1101/2019.12.20.885459; this version posted December 21, 2019. The copyright holder for this preprint (which was not certified by peer review) is the author/funder. All rights reserved. No reuse allowed without permission.

649 Biosciences) and stained with anti-CD107a (clone H4A3, BD Biosciences) for 30 minutes prior
650 to the addition of GolgiStop (1 µL/mL, BD Biosciences) and brefeldin A (BFA, 5 µg/mL, Sigma-
651 Aldrich). Costimulatory antibodies alone were used as a negative control, and concanavalin A
652 (5 µg/mL, Sigma-Aldrich) was used as a positive control. Cells were incubated for a total of 6
653 hours. After washing, cells were surface stained for CD3, CD4, and CD8, fixed/permeabilized
654 using a Cytofix/CytoPerm Kit (BD Biosciences), and stained intracellularly for IFNγ, TNFα, and
655 IL-2. The following antibodies were used: anti-CD107a–V450 (clone H4A3, BD Biosciences),
656 anti-CD3–AF700 (clone SP34-2, BD Biosciences), anti-CD4–PerCP-Cy5.5 (clone L200, BD
657 Biosciences), anti-CD8–APC-Cy7 (clone RPA-T8, BD Biosciences), anti-IFNγ–PE-Cy7 (clone
658 B27, BD Biosciences), anti-IL-2–PE (clone MQ1-17H12, BD Biosciences), and anti-TNFα–PE-
659 CF594 (clone Mab11, BD Biosciences). Data were acquired using an LSRII flow cytometer (BD
660 Biosciences) and analyzed with FlowJo software version 10 (TreeStar Inc.). Results were
661 corrected for background by subtracting the peptide stimulated response from the negative
662 (no peptide) control. Negative responses were given an arbitrary value of 0.001. All data are
663 represented. A representative flow cytometry gating strategy used to analyze cytokine
664 production via intracellular staining after peptide stimulation is shown in Figure S13.
665
666 ***MHC class I tetramer staining***
667 Biotinylated complexes of Nef RM9 (RPKVPLRTM)–Mafa A1*063:02, Gag GW9
668 (GPRKPIKCW)–Mafa A1*063:02, and Vpx GR9 (GEAFEWLNR)–Mafa B*095:01 were produced
669 as described previously*(53)*. The corresponding tetramers were generated via stepwise
670 addition of APC-conjugated streptavidin (Thermo Fisher Scientific). Frozen PBMCs were
671 stained with the pool of these tetramers for 30 minutes at 37 °C, washed, and surface
672 stained for CD3, CD4, CD8, CD14, CD20, CD27, CD45RA, CCR7, HLA-DR, and CD127. Cells

bioRxiv preprint doi: https://doi.org/10.1101/2019.12.20.885459; this version posted December 21, 2019. The copyright holder for this preprint (which was not certified by peer review) is the author/funder. All rights reserved. No reuse allowed without permission.

673 were then fixed/permeabilized using a Cytofix/CytoPerm Kit (BD Biosciences) and stained for
674 T-bet. The following antibodies were used: anti-CD3–AF700 (clone SP34-2, BD Biosciences),
675 anti-CD4–PerCP-Cy5.5 (clone L200, BD Biosciences), anti-CD8–APC-Cy7 (clone RPA-T8, BD
676 Biosciences), anti-CD14–BV786 (clone M5E2, BD Biosciences), anti-CD20–BV786 (clone L27,
677 BD Biosciences), anti-CD27–PE (clone M-T271, BD Biosciences), anti-CD45RA–PE-Cy7 (clone
678 5H9, BD Biosciences), anti-CCR7–PE-Dazzle594 (clone G043H7, BioLegend), anti-HLA-DR–
679 Pacific Blue (clone G46-6, BD Biosciences), anti-CD127–FITC (clone MB15-18C9, Miltenyi
680 Biotec), and anti-T-bet–BV711 (clone 4B10, BioLegend). Data were acquired using an AriaIII
681 flow cytometer (BD Biosciences) and analyzed with FlowJo software version 10 (TreeStar
682 Inc.). A representative flow cytometry gating strategy used to analyze T-cell differentiation
683 and tetramer staining are shown in Figure S10, S11.

684

685 ***Measurement of SIV-suppressive activity***

686 Autologous CD4$^+$ and CD8$^+$ T-cells were purified from freshly isolated PBMCs or tissue cell
687 suspensions by positive and negative selection, respectively, using antibody-coated magnetic
688 beads with a RoboSep instrument (StemCell Technologies). Purified CD4$^+$ T-cells were
689 stimulated for 3 days with concanavalin A (5µg/mL, Sigma-Aldrich) in the presence of IL-2
690 (100 IU/mL, Miltenyi Biotec). Purified CD8$^+$ T-cells were cultured in the absence of mitogens
691 and cytokines (*ex vivo* CD8$^+$ T-cells). Stimulated CD4$^+$ T-cells ($10^5$) were superinfected in U-
692 bottom 96-well plates with SIVmac251 (MOI = $10^{-3}$) in the presence (1:1 effector to target
693 cell ratio) or absence of e*x vivo* CD8$^+$ T-cells ($10^5$) from the same tissue via spinoculation for 1
694 hour (1,200 g at room temperature) followed by incubation for 1 hour at 37 °C. Cells were
695 then washed and cultured in R10 medium containing IL-2 (100 IU/mL, Miltenyi Biotec).
696 Culture supernatants were assayed on day 7 using an SIV p27 Antigen ELISA Kit

bioRxiv preprint doi: https://doi.org/10.1101/2019.12.20.885459; this version posted December 21, 2019. The copyright holder for this preprint (which was not certified by peer review) is the author/funder. All rights reserved. No reuse allowed without permission.

697 (Zeptometrix). Antiviral activity was calculated as log10 (mean p27 ng/mL in SIV-infected
698 CD4$^+$ T-cell cultures without CD8$^+$ T-cells) / (mean p27 ng/mL in SIV-infected CD4$^+$ T-cell
699 cultures + *ex vivo* CD8$^+$ T-cells) (Saez-Cirion et al., 2010).

700

701 **Data visualization and statistical analyses**

702 Data visualization was performed using Tableau version 2018.1.4 (Tableau Software).
703 Statistical analyses were performed using GraphPad version 8.1.2 (Prism Software) and
704 SigmaPlot version 12.5 (SYSTAT Software). Results are given as median with interquartile
705 range. The non-parametric Mann-Whitney U-test was used to compare data sets between
706 groups. Correlations were assessed by Spearman-rank analyses. Given the exploratory
707 nature of the analyses, p values were not adjusted for multiple comparisons. All p values less
708 than 0.05 were defined as significant.

bioRxiv preprint doi: https://doi.org/10.1101/2019.12.20.885459; this version posted December 21, 2019. The copyright holder for this preprint (which was not certified by peer review) is the author/funder. All rights reserved. No reuse allowed without permission.

709 **ACKNOWLEDGMENTS**

710 This study was funded by the French National Agency of AIDS and Viral Hepatitis Research
711 (ANRS) and by MSDAvenir. Additional support was provided by the Programme
712 Investissements d'Avenir (PIA), managed by the ANR under reference ANR-11-INBS-0008,
713 funding the Infectious Disease Models and Innovative Therapies (IDMIT, Fontenay-aux-
714 Roses, France) infrastructure, and ANR-10-EQPX-02-01, funding the FlowCyTech Facility
715 (IDMIT, Fontenay-aux-Roses, France). C.P. was supported by an ANRS Postdoctoral
716 Fellowship Grant, A.M. was supported by MSDAvenir, and D.A.P. was supported by a
717 Wellcome Trust Senior Investigator Award. We thank Benoit Delache, Brice Targat, Claire
718 Torres, Christelle Cassan, Jean-Marie Robert, Julie Morin, Patricia Brochard, Sabrina
719 Guenounou, Sebastien Langlois, and Virgile Monnet for expert technical assistance, Antonio
720 Cosma for helpful discussion, Lev Stimmer for anatomopathology expertise, Delphine
721 Desjardins and Isabelle Mangeot-Méderlé for helpful project management at IDMIT, and
722 Christophe Joubert for veterinarian assistance at the animal facility at CEA. The SIV1C cell
723 line was kindly provided by François Villinger. The SIVmac239 Gag Peptide Set was obtained
724 through the NIH AIDS Reagent Program, Division of AIDS, NIAID, NIH. FTC, DTG and TDF were
725 obtained from Gilead and ViiV healthcare though the "*IAS Towards an HIV Cure*" common
726 Material Transfer Agreement for preclinical studies in HIV cure research.

727

728 **AUTHOR CONTRIBUTIONS**

729 C.P. and A.M. designed and performed experiments, analyzed data, and interpreted results.
730 V.Ma., J.G., and V.A.F. analyzed data and interpreted results. V.Mo., A.D., P.V., and N.S.
731 performed experiments and analyzed data. E.G. and D.A.P. produced bespoke reagents.
732 N.D.B. designed experiments, analyzed data and interpreted results. D.A.P., A.B., G.P., R.L.G.,

bioRxiv preprint doi: https://doi.org/10.1101/2019.12.20.885459; this version posted December 21, 2019. The copyright holder for this preprint (which was not certified by peer review) is the author/funder. All rights reserved. No reuse allowed without permission.

733 O.L., M.M.T., and C.R. interpreted results. B.V. and A.S.C. designed experiments, analyzed
734 data, interpreted results, and supervised the study. C.P., B.V., and A.S.C. wrote the paper
735 with assistance from A.M., V.Ma., V.Mo., A.D., P.V., N.S., D.A.P., N.D.B., R.L.G., O.L., M.M.T.,
736 C.R., J.G., and V.A.F.

737

738 **DECLARATION OF INTERESTS**

739 The authors declare no competing interests.

bioRxiv preprint doi: https://doi.org/10.1101/2019.12.20.885459; this version posted December 21, 2019. The copyright holder for this preprint (which was not certified by peer review) is the author/funder. All rights reserved. No reuse allowed without permission.

740 **REFERENCES**


741 Aarnink, A., Dereuddre-Bosquet, N., Vaslin, B., Le Grand, R., Winterton, P., Apoil, P.A., and
742 Blancher, A. (2011). Influence of the MHC genotype on the progression of experimental SIV
743 infection in the Mauritian cynomolgus macaque. Immunogenetics *63*, 267-274.
744 Allen, T.M., O'Connor, D.H., Jing, P., Dzuris, J.L., Mothe, B.R., Vogel, T.U., Dunphy, E.,
745 Liebl, M.E., Emerson, C., Wilson, N.*, et al.* (2000). Tat-specific cytotoxic T lymphocytes
746 select for SIV escape variants during resolution of primary viraemia. Nature *407*, 386-390.
747 Almeida, J.R., Price, D.A., Papagno, L., Arkoub, Z.A., Sauce, D., Bornstein, E., Asher, T.E.,
748 Samri, A., Schnuriger, A., Theodorou, I.*, et al.* (2007). Superior control of HIV-1 replication by
749 CD8+ T cells is reflected by their avidity, polyfunctionality, and clonal turnover. J Exp Med
750 *204*, 2473-2485.
751 Almeida, J.R., Sauce, D., Price, D.A., Papagno, L., Shin, S.Y., Moris, A., Larsen, M.,
752 Pancino, G., Douek, D.C., Autran, B.*, et al.* (2009). Antigen sensitivity is a major determinant
753 of CD8+ T-cell polyfunctionality and HIV-suppressive activity. Blood *113*, 6351-6360.
754 Angin, M., Volant, S., Passaes, C., Lecuroux, C., Monceaux, V., Dillies, M.-A., Valle-Casuso,
755 J., Pancino, G., Vaslin, B., Le Grand, R.*, et al.* (2019a). Metabolic plasticity of HIV-specific
756 CD8+ T cells is associated with enhanced antiviral potential and natural control of HIV-1
757 infection. Nature Metabolism.
758 Angin, M., Volant, S., Passaes, C., Lecuroux, C., Monceaux, V., Dillies, M.-A., Valle-Casuso,
759 J.C., Pancino, G., Vaslin, B., Grand, R.L.*, et al.* (2019b). Metabolic plasticity of HIV-specific
760 CD8+ T cells is associated with enhanced antiviral potential and natural control of HIV-1
761 infection. Nature Metabolism *1*, 704-716.
762 Angin, M., Wong, G., Papagno, L., Versmisse, P., David, A., Bayard, C., Charmeteau-De
763 Muylder, B., Besseghir, A., Thiebaut, R., Boufassa, F.*, et al.* (2016). Preservation of
764 Lymphopoietic Potential and Virus Suppressive Capacity by CD8+ T Cells in HIV-2-Infected
765 Controllers. J Immunol *197*, 2787-2795.
766 Antony, J.M., and MacDonald, K.S. (2015). A critical analysis of the cynomolgus macaque,
767 Macaca fascicularis, as a model to test HIV-1/SIV vaccine efficacy. Vaccine *33*, 3073-3083.
768 Barouch, D.H., Ghneim, K., Bosche, W.J., Li, Y., Berkemeier, B., Hull, M., Bhattacharyya, S.,
769 Cameron, M., Liu, J., Smith, K.*, et al.* (2016). Rapid Inflammasome Activation following
770 Mucosal SIV Infection of Rhesus Monkeys. Cell *165*, 656-667.
771 Betts, M.R., Nason, M.C., West, S.M., De Rosa, S.C., Migueles, S.A., Abraham, J.,
772 Lederman, M.M., Benito, J.M., Goepfert, P.A., Connors, M.*, et al.* (2006). HIV
773 nonprogressors preferentially maintain highly functional HIV-specific CD8+ T cells. Blood
774 *107*, 4781-4789.
775 Borrow, P., Lewicki, H., Hahn, B.H., Shaw, G.M., and Oldstone, M.B. (1994). Virus-specific
776 CD8+ cytotoxic T-lymphocyte activity associated with control of viremia in primary human
777 immunodeficiency virus type 1 infection. J Virol *68*, 6103-6110.
778 Borrow, P., Lewicki, H., Wei, X., Horwitz, M.S., Peffer, N., Meyers, H., Nelson, J.A., Gairin,
779 J.E., Hahn, B.H., Oldstone, M.B.*, et al.* (1997). Antiviral pressure exerted by HIV-1-specific
780 cytotoxic T lymphocytes (CTLs) during primary infection demonstrated by rapid selection of
781 CTL escape virus. Nat Med *3*, 205-211.
782 Bruel, T., Hamimi, C., Dereuddre-Bosquet, N., Cosma, A., Shin, S.Y., Corneau, A.,
783 Versmisse, P., Karlsson, I., Malleret, B., Targat, B.*, et al.* (2015). Long-term control of simian
784 immunodeficiency virus (SIV) in cynomolgus macaques not associated with efficient SIV-
785 specific CD8+ T-cell responses. J Virol *89*, 3542-3556.
786 Buckheit, R.W., 3rd, Salgado, M., Silciano, R.F., and Blankson, J.N. (2012). Inhibitory
787 potential of subpopulations of CD8+ T cells in HIV-1-infected elite suppressors. J Virol *86*,
788 13679-13688.
789 Budde, M.L., Wiseman, R.W., Karl, J.A., Hanczaruk, B., Simen, B.B., and O'Connor, D.H.
790 (2010). Characterization of Mauritian cynomolgus macaque major histocompatibility complex
791 class I haplotypes by high-resolution pyrosequencing. Immunogenetics *62*, 773-780.
792 Buggert, M., Nguyen, S., Salgado-Montes de Oca, G., Bengsch, B., Darko, S., Ransier, A.,
793 Roberts, E.R., Del Alcazar, D., Brody, I.B., Vella, L.A.*, et al.* (2018). Identification and

bioRxiv preprint doi: https://doi.org/10.1101/2019.12.20.885459; this version posted December 21, 2019. The copyright holder for this preprint (which was not certified by peer review) is the author/funder. All rights reserved. No reuse allowed without permission.

794 characterization of HIV-specific resident memory CD8(+) T cells in human lymphoid tissue.
795 Sci Immunol *3*.
796 Busch, D.H., and Pamer, E.G. (1999). T cell affinity maturation by selective expansion during
797 infection. J Exp Med *189*, 701-710.
798 Carrington, M., Nelson, G.W., Martin, M.P., Kissner, T., Vlahov, D., Goedert, J.J., Kaslow, R.,
799 Buchbinder, S., Hoots, K., and O'Brien, S.J. (1999). HLA and HIV-1: heterozygote advantage
800 and B*35-Cw*04 disadvantage. Science *283*, 1748-1752.
801 Chowdhury, A., Hayes, T.L., Bosinger, S.E., Lawson, B.O., Vanderford, T., Schmitz, J.E.,
802 Paiardini, M., Betts, M., Chahroudi, A., Estes, J.D.*, et al.* (2015). Differential Impact of In Vivo
803 CD8+ T Lymphocyte Depletion in Controller versus Progressor Simian Immunodeficiency
804 Virus-Infected Macaques. J Virol *89*, 8677-8686.
805 Day, C.L., Kaufmann, D.E., Kiepiela, P., Brown, J.A., Moodley, E.S., Reddy, S., Mackey,
806 E.W., Miller, J.D., Leslie, A.J., DePierres, C.*, et al.* (2006). PD-1 expression on HIV-specific T
807 cells is associated with T-cell exhaustion and disease progression. Nature *443*, 350-354.
808 Du, V.Y., Bansal, A., Carlson, J., Salazar-Gonzalez, J.F., Salazar, M.G., Ladell, K., Gras, S.,
809 Josephs, T.M., Heath, S.L., Price, D.A.*, et al.* (2016). HIV-1-Specific CD8 T Cells Exhibit
810 Limited Cross-Reactivity during Acute Infection. J Immunol *196*, 3276-3286.
811 Feichtinger, H., Putkonen, P., Parravicini, C., Li, S.L., Kaaya, E.E., Bottiger, D., Biberfeld, G.,
812 and Biberfeld, P. (1990). Malignant lymphomas in cynomolgus monkeys infected with simian
813 immunodeficiency virus. Am J Pathol *137*, 1311-1315.
814 Hersperger, A.R., Martin, J.N., Shin, L.Y., Sheth, P.M., Kovacs, C.M., Cosma, G.L.,
815 Makedonas, G., Pereyra, F., Walker, B.D., Kaul, R.*, et al.* (2011a). Increased HIV-specific
816 CD8+ T-cell cytotoxic potential in HIV elite controllers is associated with T-bet expression.
817 Blood *117*, 3799-3808.
818 Hersperger, A.R., Migueles, S.A., Betts, M.R., and Connors, M. (2011b). Qualitative features
819 of the HIV-specific CD8+ T-cell response associated with immunologic control. Curr Opin HIV
820 AIDS *6*, 169-173.
821 Hersperger, A.R., Pereyra, F., Nason, M., Demers, K., Sheth, P., Shin, L.Y., Kovacs, C.M.,
822 Rodriguez, B., Sieg, S.F., Teixeira-Johnson, L.*, et al.* (2010). Perforin expression directly ex
823 vivo by HIV-specific CD8 T-cells is a correlate of HIV elite control. PLoS Pathog *6*,
824 e1000917.
825 Joshi, N.S., Cui, W., Chandele, A., Lee, H.K., Urso, D.R., Hagman, J., Gapin, L., and Kaech,
826 S.M. (2007). Inflammation directs memory precursor and short-lived effector CD8(+) T cell
827 fates via the graded expression of T-bet transcription factor. Immunity *27*, 281-295.
828 Joshi, N.S., Cui, W., Dominguez, C.X., Chen, J.H., Hand, T.W., and Kaech, S.M. (2011).
829 Increased numbers of preexisting memory CD8 T cells and decreased T-bet expression can
830 restrain terminal differentiation of secondary effector and memory CD8 T cells. J Immunol
831 *187*, 4068-4076.
832 Julg, B., Williams, K.L., Reddy, S., Bishop, K., Qi, Y., Carrington, M., Goulder, P.J., Ndung'u,
833 T., and Walker, B.D. (2010). Enhanced anti-HIV functional activity associated with Gag-
834 specific CD8 T-cell responses. J Virol *84*, 5540-5549.
835 Karlsson, I., Malleret, B., Brochard, P., Delache, B., Calvo, J., Le Grand, R., and Vaslin, B.
836 (2007). Dynamics of T-cell responses and memory T cells during primary simian
837 immunodeficiency virus infection in cynomolgus macaques. J Virol *81*, 13456-13468.
838 Khanolkar, A., Fuller, M.J., and Zajac, A.J. (2004). CD4 T cell-dependent CD8 T cell
839 maturation. J Immunol *172*, 2834-2844.
840 Koup, R.A., Safrit, J.T., Cao, Y., Andrews, C.A., McLeod, G., Borkowsky, W., Farthing, C.,
841 and Ho, D.D. (1994). Temporal association of cellular immune responses with the initial
842 control of viremia in primary human immunodeficiency virus type 1 syndrome. J Virol *68*,
843 4650-4655.
844 Ladell, K., Hashimoto, M., Iglesias, M.C., Wilmann, P.G., McLaren, J.E., Gras, S., Chikata,
845 T., Kuse, N., Fastenackels, S., Gostick, E.*, et al.* (2013). A molecular basis for the control of
846 preimmune escape variants by HIV-specific CD8+ T cells. Immunity *38*, 425-436.
847 Lecuroux, C., Girault, I., Cheret, A., Versmisse, P., Nembot, G., Meyer, L., Rouzioux, C.,
848 Pancino, G., Venet, A., Saez-Cirion, A.*, et al.* (2013). CD8 T-cells from most HIV-infected

bioRxiv preprint doi: https://doi.org/10.1101/2019.12.20.885459; this version posted December 21, 2019. The copyright holder for this preprint (which was not certified by peer review) is the author/funder. All rights reserved. No reuse allowed without permission.

849 patients lack ex vivo HIV-suppressive capacity during acute and early infection. PLoS One *8*,
850 e59767.
851 Lecuroux, C., Saez-Cirion, A., Girault, I., Versmisse, P., Boufassa, F., Avettand-Fenoel, V.,
852 Rouzioux, C., Meyer, L., Pancino, G., Lambotte, O.*, et al.* (2014). Both HLA-B*57 and
853 plasma HIV RNA levels contribute to the HIV-specific CD8+ T cell response in HIV
854 controllers. J Virol *88*, 176-187.
855 Mannioui, A., Bourry, O., Sellier, P., Delache, B., Brochard, P., Andrieu, T., Vaslin, B.,
856 Karlsson, I., Roques, P., and Le Grand, R. (2009). Dynamics of viral replication in blood and
857 lymphoid tissues during SIVmac251 infection of macaques. Retrovirology *6*, 106.
858 McBrien, J.B., Kumar, N.A., and Silvestri, G. (2018). Mechanisms of CD8(+) T cell-mediated
859 suppression of HIV/SIV replication. Eur J Immunol *48*, 898-914.
860 Mee, E.T., Berry, N., Ham, C., Sauermann, U., Maggiorella, M.T., Martinon, F., Verschoor,
861 E.J., Heeney, J.L., Le Grand, R., Titti, F.*, et al.* (2009). Mhc haplotype H6 is associated with
862 sustained control of SIVmac251 infection in Mauritian cynomolgus macaques.
863 Immunogenetics *61*, 327-339.
864 Migueles, S.A., Laborico, A.C., Shupert, W.L., Sabbaghian, M.S., Rabin, R., Hallahan, C.W.,
865 Van Baarle, D., Kostense, S., Miedema, F., McLaughlin, M.*, et al.* (2002). HIV-specific CD8+
866 T cell proliferation is coupled to perforin expression and is maintained in nonprogressors. Nat
867 Immunol *3*, 1061-1068.
868 Migueles, S.A., Osborne, C.M., Royce, C., Compton, A.A., Joshi, R.P., Weeks, K.A., Rood,
869 J.E., Berkley, A.M., Sacha, J.B., Cogliano-Shutta, N.A.*, et al.* (2008). Lytic granule loading of
870 CD8+ T cells is required for HIV-infected cell elimination associated with immune control.
871 Immunity *29*, 1009-1021.
872 Migueles, S.A., Sabbaghian, M.S., Shupert, W.L., Bettinotti, M.P., Marincola, F.M., Martino,
873 L., Hallahan, C.W., Selig, S.M., Schwartz, D., Sullivan, J.*, et al.* (2000). HLA B*5701 is highly
874 associated with restriction of virus replication in a subgroup of HIV-infected long term
875 nonprogressors. Proc Natl Acad Sci U S A *97*, 2709-2714.
876 Ndhlovu, Z.M., Kamya, P., Mewalal, N., Kloverpris, H.N., Nkosi, T., Pretorius, K., Laher, F.,
877 Ogunshola, F., Chopera, D., Shekhar, K.*, et al.* (2015). Magnitude and Kinetics of CD8+ T
878 Cell Activation during Hyperacute HIV Infection Impact Viral Set Point. Immunity *43*, 591-604.
879 Noel, N., Pena, R., David, A., Avettand-Fenoel, V., Erkizia, I., Jimenez, E., Lecuroux, C.,
880 Rouzioux, C., Boufassa, F., Pancino, G.*, et al.* (2016). Long-Term Spontaneous Control of
881 HIV-1 Is Related to Low Frequency of Infected Cells and Inefficient Viral Reactivation. J Virol
882 *90*, 6148-6158.
883 O'Connor, D.H., Allen, T.M., Vogel, T.U., Jing, P., DeSouza, I.P., Dodds, E., Dunphy, E.J.,
884 Melsaether, C., Mothe, B., Yamamoto, H.*, et al.* (2002). Acute phase cytotoxic T lymphocyte
885 escape is a hallmark of simian immunodeficiency virus infection. Nat Med *8*, 493-499.
886 O'Connor, S.L., Lhost, J.J., Becker, E.A., Detmer, A.M., Johnson, R.C., Macnair, C.E.,
887 Wiseman, R.W., Karl, J.A., Greene, J.M., Burwitz, B.J.*, et al.* (2010). MHC heterozygote
888 advantage in simian immunodeficiency virus-infected Mauritian cynomolgus macaques. Sci
889 Transl Med *2*, 22ra18.
890 Ozga, A.J., Moalli, F., Abe, J., Swoger, J., Sharpe, J., Zehn, D., Kreutzfeldt, M., Merkler, D.,
891 Ripoll, J., and Stein, J.V. (2016). pMHC affinity controls duration of CD8+ T cell-DC
892 interactions and imprints timing of effector differentiation versus expansion. J Exp Med *213*,
893 2811-2829.
894 Pereyra, F., Addo, M.M., Kaufmann, D.E., Liu, Y., Miura, T., Rathod, A., Baker, B., Trocha,
895 A., Rosenberg, R., Mackey, E.*, et al.* (2008). Genetic and immunologic heterogeneity among
896 persons who control HIV infection in the absence of therapy. J Infect Dis *197*, 563-571.
897 Petrovas, C., Casazza, J.P., Brenchley, J.M., Price, D.A., Gostick, E., Adams, W.C.,
898 Precopio, M.L., Schacker, T., Roederer, M., Douek, D.C.*, et al.* (2006). PD-1 is a regulator of
899 virus-specific CD8+ T cell survival in HIV infection. J Exp Med *203*, 2281-2292.
900 Petrovas, C., Price, D.A., Mattapallil, J., Ambrozak, D.R., Geldmacher, C., Cecchinato, V.,
901 Vaccari, M., Tryniszewska, E., Gostick, E., Roederer, M.*, et al.* (2007). SIV-specific CD8+ T
902 cells express high levels of PD1 and cytokines but have impaired proliferative capacity in
903 acute and chronic SIVmac251 infection. Blood *110*, 928-936.

bioRxiv preprint doi: https://doi.org/10.1101/2019.12.20.885459; this version posted December 21, 2019. The copyright holder for this preprint (which was not certified by peer review) is the author/funder. All rights reserved. No reuse allowed without permission.

904 Price, D.A., Brenchley, J.M., Ruff, L.E., Betts, M.R., Hill, B.J., Roederer, M., Koup, R.A.,
905 Migueles, S.A., Gostick, E., Wooldridge, L., *et al.* (2005). Avidity for antigen shapes clonal
906 dominance in CD8+ T cell populations specific for persistent DNA viruses. J Exp Med *202*,
907 1349-1361.
908 Price, D.A., Goulder, P.J., Klenerman, P., Sewell, A.K., Easterbrook, P.J., Troop, M.,
909 Bangham, C.R., and Phillips, R.E. (1997). Positive selection of HIV-1 cytotoxic T lymphocyte
910 escape variants during primary infection. Proc Natl Acad Sci U S A *94*, 1890-1895.
911 Putkonen, P., Warstedt, K., Thorstensson, R., Benthin, R., Albert, J., Lundgren, B., Oberg,
912 B., Norrby, E., and Biberfeld, G. (1989). Experimental infection of cynomolgus monkeys
913 (Macaca fascicularis) with simian immunodeficiency virus (SIVsm). J Acquir Immune Defic
914 Syndr *2*, 359-365.
915 Rao, R.R., Li, Q., Gubbels Bupp, M.R., and Shrikant, P.A. (2012). Transcription factor Foxo1
916 represses T-bet-mediated effector functions and promotes memory CD8(+) T cell
917 differentiation. Immunity *36*, 374-387.
918 Reuter, M.A., Del Rio Estrada, P.M., Buggert, M., Petrovas, C., Ferrando-Martinez, S.,
919 Nguyen, S., Sada Japp, A., Ablanedo-Terrazas, Y., Rivero-Arrieta, A., Kuri-Cervantes, L., *et*
920 *al.* (2017). HIV-Specific CD8(+) T Cells Exhibit Reduced and Differentially Regulated
921 Cytolytic Activity in Lymphoid Tissue. Cell Rep *21*, 3458-3470.
922 Saez-Cirion, A., Bacchus, C., Hocqueloux, L., Avettand-Fenoel, V., Girault, I., Lecuroux, C.,
923 Potard, V., Versmisse, P., Melard, A., Prazuck, T., *et al.* (2013). Post-treatment HIV-1
924 controllers with a long-term virological remission after the interruption of early initiated
925 antiretroviral therapy ANRS VISCONTI Study. PLoS Pathog *9*, e1003211.
926 Saez-Cirion, A., Lacabaratz, C., Lambotte, O., Versmisse, P., Urrutia, A., Boufassa, F.,
927 Barre-Sinoussi, F., Delfraissy, J.F., Sinet, M., Pancino, G., *et al.* (2007). HIV controllers
928 exhibit potent CD8 T cell capacity to suppress HIV infection ex vivo and peculiar cytotoxic T
929 lymphocyte activation phenotype. Proc Natl Acad Sci U S A *104*, 6776-6781.
930 Saez-Cirion, A., and Pancino, G. (2013). HIV controllers: a genetically determined or
931 inducible phenotype? Immunol Rev *254*, 281-294.
932 Saez-Cirion, A., Shin, S.Y., Versmisse, P., Barre-Sinoussi, F., and Pancino, G. (2010). Ex
933 vivo T cell-based HIV suppression assay to evaluate HIV-specific CD8+ T-cell responses.
934 Nat Protoc *5*, 1033-1041.
935 Saez-Cirion, A., Sinet, M., Shin, S.Y., Urrutia, A., Versmisse, P., Lacabaratz, C., Boufassa,
936 F., Avettand-Fenoel, V., Rouzioux, C., Delfraissy, J.F., *et al.* (2009). Heterogeneity in HIV
937 suppression by CD8 T cells from HIV controllers: association with Gag-specific CD8 T cell
938 responses. J Immunol *182*, 7828-7837.
939 Schluns, K.S., Kieper, W.C., Jameson, S.C., and Lefrancois, L. (2000). Interleukin-7
940 mediates the homeostasis of naive and memory CD8 T cells in vivo. Nat Immunol *1*, 426-
941 432.
942 Simonetta, F., Hua, S., Lecuroux, C., Gerard, S., Boufassa, F., Saez-Cirion, A., Pancino, G.,
943 Goujard, C., Lambotte, O., Venet, A., *et al.* (2014). High eomesodermin expression among
944 CD57+ CD8+ T cells identifies a CD8+ T cell subset associated with viral control during
945 chronic human immunodeficiency virus infection. J Virol *88*, 11861-11871.
946 Snell, L.M., MacLeod, B.L., Law, J.C., Osokine, I., Elsaesser, H.J., Hezaveh, K., Dickson,
947 R.J., Gavin, M.A., Guidos, C.J., McGaha, T.L., *et al.* (2018). CD8(+) T Cell Priming in
948 Established Chronic Viral Infection Preferentially Directs Differentiation of Memory-like Cells
949 for Sustained Immunity. Immunity *49*, 678-694 e675.
950 Sullivan, B.M., Juedes, A., Szabo, S.J., von Herrath, M., and Glimcher, L.H. (2003). Antigen-
951 driven effector CD8 T cell function regulated by T-bet. Proc Natl Acad Sci U S A *100*, 15818-
952 15823.
953 Szabo, S.J., Sullivan, B.M., Stemmann, C., Satoskar, A.R., Sleckman, B.P., and Glimcher,
954 L.H. (2002). Distinct effects of T-bet in TH1 lineage commitment and IFN-gamma production
955 in CD4 and CD8 T cells. Science *295*, 338-342.
956 Takata, H., Buranapraditkun, S., Kessing, C., Fletcher, J.L., Muir, R., Tardif, V., Cartwright,
957 P., Vandergeeten, C., Bakeman, W., Nichols, C.N., *et al.* (2017). Delayed differentiation of

bioRxiv preprint doi: https://doi.org/10.1101/2019.12.20.885459; this version posted December 21, 2019. The copyright holder for this preprint (which was not certified by peer review) is the author/funder. All rights reserved. No reuse allowed without permission.

958 potent effector CD8(+) T cells reducing viremia and reservoir seeding in acute HIV infection.
959 Sci Transl Med *9*.
960 Takemoto, N., Intlekofer, A.M., Northrup, J.T., Wherry, E.J., and Reiner, S.L. (2006). Cutting
961 Edge: IL-12 inversely regulates T-bet and eomesodermin expression during pathogen-
962 induced CD8+ T cell differentiation. J Immunol *177*, 7515-7519.
963 Tansiri, Y., Rowland-Jones, S.L., Ananworanich, J., and Hansasuta, P. (2015). Clinical
964 outcome of HIV viraemic controllers and noncontrollers with normal CD4 counts is
965 exclusively determined by antigen-specific CD8+ T-cell-mediated HIV suppression. PLoS
966 One *10*, e0118871.
967 Trautmann, L., Janbazian, L., Chomont, N., Said, E.A., Gimmig, S., Bessette, B., Boulassel,
968 M.R., Delwart, E., Sepulveda, H., Balderas, R.S., *et al.* (2006). Upregulation of PD-1
969 expression on HIV-specific CD8+ T cells leads to reversible immune dysfunction. Nat Med
970 *12*, 1198-1202.
971 Trautmann, L., Mbitikon-Kobo, F.M., Goulet, J.P., Peretz, Y., Shi, Y., Van Grevenynghe, J.,
972 Procopio, F.A., Boulassel, M.R., Routy, J.P., Chomont, N., *et al.* (2012). Profound metabolic,
973 functional, and cytolytic differences characterize HIV-specific CD8 T cells in primary and
974 chronic HIV infection. Blood *120*, 3466-3477.
975 Walker, B., and McMichael, A. (2012). The T-cell response to HIV. Cold Spring Harb
976 Perspect Med *2*.
977 Zimmerli, S.C., Harari, A., Cellerai, C., Vallelian, F., Bart, P.A., and Pantaleo, G. (2005). HIV-
978 1-specific IFN-gamma/IL-2-secreting CD8 T cells support CD4-independent proliferation of
979 HIV-1-specific CD8 T cells. Proc Natl Acad Sci U S A *102*, 7239-7244.
980

981

bioRxiv preprint doi: https://doi.org/10.1101/2019.12.20.885459; this version posted December 21, 2019. The copyright holder for this preprint (which was not certified by peer review) is the author/funder. All rights reserved. No reuse allowed without permission.

982 **FIGURE LEGENDS**

983 **Figure 1. SIV controllers are characterized by partial restoration of CD4$^+$ T-cell counts and**
984 **progressive decline in the frequency of SIV-carrying cells in blood.** (**A**) Plasma VL kinetics,
985 (**B**) kinetics of SIV-DNA levels in blood and (**C**) longitudinal evolution of CD4$^+$ T-cell counts
986 (results are shown as fold-change in absolute CD4$^+$ T-cell counts relative to baseline) in blood
987 in SIV controllers (SICs, black) and viremic CyMs (VIRs, red). Median and interquartile range
988 are shown. *p < 0.05, **p < 0.01, ***p < 0.001; Mann-Whitney U-test.

989

990 **Figure 2. SIV control is associated with early preservation of lymph nodes.** (**A**–**B**)
991 Longitudinal evolution of CD4$^+$ T-cells in rectal mucosa (**A**), and peripheral lymph nodes (**B**) in
992 SIV controllers (SICs, black) and viremic CyMs (VIRs, red). Results in rectal mucosa and
993 peripheral lymph nodes are shown as fold-change in percent frequencies of CD3$^+$ CD4$^+$ T-
994 cells among CD3$^+$ lymphocytes relative to baseline. (**C**) Percent frequencies of CD3$^+$ CD4$^+$ T-
995 cells among CD3$^+$ lymphocytes in bone marrow, spleen, peripheral and mesenteric lymph
996 nodes, and colon mucosa at euthanasia. (**D**–**E**) Kinetics of SIV-DNA levels in rectal mucosa
997 (**D**), and peripheral lymph nodes (**E**) in SIV controllers (black) and viremic CyMs (red). (**F**)
998 Levels of SIV-DNA in bone marrow, spleen, peripheral and mesenteric lymph nodes, and
999 colon at euthanasia. Results are expressed as copies SIV-DNA/million CD4$^+$ T-cells. Median
1000 and interquartile range are shown. *p < 0.05, **p < 0.01; Mann-Whitney U-test.

1001

1002 **Figure 3. The dynamics of CD8$^+$ T-cells expansion and activation do not predict control of**
1003 **SIV.** (**A**–**C**) Evolution of Ki-67$^+$ CD8$^+$ T-cells in blood (**A**), peripheral lymph nodes (**B**), and
1004 rectal mucosa (**C**) in SIV controllers (black) and viremic CyMs (red). (**D**–**F**) Evolution of CD38$^+$
1005 HLA-DR$^+$ CD8$^+$ T-cells in blood (**D**), peripheral lymph nodes (**E**), and rectal mucosa (**F**) in SIV

bioRxiv preprint doi: https://doi.org/10.1101/2019.12.20.885459; this version posted December 21, 2019. The copyright holder for this preprint (which was not certified by peer review) is the author/funder. All rights reserved. No reuse allowed without permission.

1006 controllers (black) and viremic CyMs (red). Median and interquartile range are shown.
1007 Vertical dashed lines indicate peak VLs. *p < 0.05, **p < 0.01; Mann-Whitney U-test.
1008
1009 **Figure 4. SIV-specific CD8$^+$ T-cell frequencies do not predict control of SIV.** (**A**) TNF$\alpha$
1010 production by SIV-specific CD8$^+$ T-cells in blood and peripheral lymph nodes over the course
1011 of infection and in bone marrow, spleen, and mesenteric lymph nodes at euthanasia in SIV
1012 controllers (black) and viremic CyMs (red). Results are shown as percent frequencies among
1013 CD8$^+$ T-cells. Median and interquartile range are shown. (**B**) Functional profiles of SIV-specific
1014 CD8$^+$ T-cells in blood and peripheral lymph nodes over the course of infection and in bone
1015 marrow, spleen, and mesenteric lymph nodes at euthanasia in SIV controllers (black) and
1016 viremic CyMs (red). Doughnut charts show median percent frequencies of SIV-specific CD8$^+$
1017 T-cells expressing IFN$\gamma$, TNF$\alpha$, IL-2, and/or CD107a. Colors indicate number of simultaneous
1018 functions (blue, 1; green, 2; yellow, 3; red, 4). *p < 0.05; Mann-Whitney U-test.
1019
1020 **Figure 5. Progressive acquisition of CD8$^+$ T-cell-mediated SIV-suppressive activity is**
1021 **associated with control of SIV.** (**A**) CD8$^+$ T-cell-mediated SIV-suppressive activity in blood
1022 and peripheral lymph nodes over the course of infection and in bone marrow, spleen, and
1023 mesenteric lymph nodes at euthanasia in SIV controllers (black) and viremic CyMs (red).
1024 Results are shown as log p27 decrease in the presence of CD8$^+$ T-cells. *p < 0.05, **p < 0.01;
1025 Mann-Whitney U-test. (**B**) Spearman correlations between CD8$^+$ T-cell-mediated SIV-
1026 suppressive activity (upper panel) or TNF$\alpha$ production by SIV-specific CD8$^+$ T-cells (bottom
1027 panel) on day 15 *p.i.* with plasma VL on day 15 *p.i.* Grey symbols, SIV controllers; red
1028 symbols, viremic CyMs. (**C**) Spearman correlations between CD8$^+$ T-cell-mediated SIV-
1029 suppressive activity (upper panel) or TNF$\alpha$ production by SIV-specific CD8$^+$ T-cells (bottom

bioRxiv preprint doi: https://doi.org/10.1101/2019.12.20.885459; this version posted December 21, 2019. The copyright holder for this preprint (which was not certified by peer review) is the author/funder. All rights reserved. No reuse allowed without permission.

1030 panel) at euthanasia with plasma VL at euthanasia. Grey symbols, SIV controllers; red
1031 symbols, viremic CyMs (**D**) Spearman correlations between area under the curve (AUC) for
1032 plasma VL and AUC for CD8$^+$ T-cell-mediated SIV-suppressive activity (orange) and between
1033 AUC for plasma VL and AUC for TNF$\alpha$ production by SIV-specific CD8$^+$ T-cells (blue). AUC for
1034 plasma VL, TNF$\alpha$ production and CD8+ T-cell antiviral activities were calculated using the
1035 sequential values obtained throughout the duration of our study in the blood of the infected
1036 animals (Figure S6). (**E**) Side by side comparison of the longitudinal kinetics of TNF$\alpha$
1037 production by SIV-specific CD8$^+$ T-cells in blood shown in figure 4A (blue) and CD8$^+$ T-cell-
1038 mediated SIV-suppressive activity in blood shown in figure 5A(orange) in SIV controllers (left
1039 panel) and viremic CyMs (right panel). Median and interquartile range are shown.
1040
1041 **Figure 6. SIV controllers maintain higher frequencies of SIV-specific central memory CD8$^+$**
1042 **T-cells during chronic infection than viremic CyMs.** (**A**) Doughnut charts showing median
1043 percent frequencies of SIV-specific CD8$^+$ T-cells in each phenotypically-defined subset in SIV
1044 controllers (upper panels) and viremic CyMs (lower panels). Light blue, central memory
1045 (CM); green, transitional memory (TM); yellow, effector memory (EM); red, effector (Eff). (**B**)
1046 Evolution of CM, TM, EM, and Eff SIV-specific CD8$^+$ T-cells in SIV controllers (black) and
1047 viremic CyMs (red). Results are shown as percent frequencies of tetramer-binding CD8$^+$ T-
1048 cells. *$p < 0.05$; Mann-Whitney U-test.
1049
1050 **Figure 7. Altered maturation of central memory SIV-specific CD8$^+$ T-cells in viremic CyMs.**
1051 (**A**) Dynamics of T-bet (left panels) and CD127 expression (right panels) among SIV-specific
1052 CD8$^+$ T-cells in SIV controllers (black) and viremic CyMs (red). (**B**) Dynamics of T-bet (left) and
1053 CD127 expression (right) among central memory (CM), transitional memory (TM), effector

bioRxiv preprint doi: https://doi.org/10.1101/2019.12.20.885459; this version posted December 21, 2019. The copyright holder for this preprint (which was not certified by peer review) is the author/funder. All rights reserved. No reuse allowed without permission.

1054 memory (EM), and effector (Eff) SIV-specific $CD8^+$ T-cells in SIV controllers (black) and
1055 viremic CyMs (red). *p < 0.05, **p < 0.01; Mann-Whitney U-test.
1056
1057 **Figure 8. Skewed maturation of central memory SIV-specific $CD8^+$ T-cells is associated with**
1058 **defective acquisition of SIV-suppressive activity.** Spearman correlations between CD127+
1059 SIV specific $CD8^+$ T cell frequencies and viral loads (**A**) and $CD8^+$ T-cell-mediated SIV-
1060 suppressive activity (**B**) during acute (left panel) and chronic infection (right panel).
1061 Spearman correlations between T-bet$^+$ CD127$^-$ SIV-specific $CD8^+$ T-cell frequencies (**C**) or T-
1062 bet expression levels in central memory SIV-specific $CD8^+$ T-cells (**D**) and $CD8^+$ T-cell-
1063 mediated SIV-suppressive activity during acute (left panel) and chronic infection (right
1064 panel). Grey symbols, SIV controllers; red symbols, viremic CyMs.

bioRxiv preprint doi: https://doi.org/10.1101/2019.12.20.885459; this version posted December 21, 2019. The copyright holder for this preprint (which was not certified by peer review) is the author/funder. All rights reserved. No reuse allowed without permission.

1065 **Table 1.** Virologic and immunologic characteristics from SICs *versus* VIRs.

| | Controllers | Viremics | p |
|---|---|---|---|
| **RNA viral load** | | | |
| Peak (Log SIV-RNA copies/mL) | 6.1 [5.1 – 7.1] | 6.6 [6.3 – 6.9] | 0.058 |
| Time to peak (days *p.i.*) | 12.5 [11 – 17] | 14 [14 – 17] | 0.239 |
| Set-point# (Log SIV-RNA copies/mL) | 1.5 [1.1 – 3.6] | 4.0 [3.2 – 5.2] | **0.014** |
| Slope after peak viremia (1/slope peak – set-point) | $-1.3 \times 10^{-4}$ [$-1.5 \times 10^{-3}$ to $-2.1 \times 10^{-5}$] | $-5.5 \times 10^{-5}$ [$-1.2 \times 10^{-4}$ to $-2.3 \times 10^{-5}$] | 0.058 |
| **DNA viral load** | | | |
| Peak (Log SIV-DNA copies/million CD4) | 4.0 [3.5 – 4.7] | 4.6 [4.1 – 5.3] | 0.133 |
| Time to peak (days *p.i.*) | 15 [15 – 36] | 15 [15 – 36] | 1 |
| Set-point# (Log SIV-DNA copies/million CD4) | 2.7 [2.1 – 3.5] | 4.0 [3.8 – 4.5] | **0.002** |
| Descending slope (1/slope peak – set-point) | $-9.0 \times 10^{-3}$ [$-4.8 \times 10^{-2}$ to $-1.0 \times 10^{-3}$] | $-4.9 \times 10^{-3}$ [$-1.2 \times 10^{-2}$ to $-4.4 \times 10^{-4}$] | 0.262 |
| **$CD4^+$ T-cell counts** | | | |
| Nadir $CD4^+$ T-cells (cells/µL blood) | 238 [71 – 910] | 179 [73 – 276] | 0.379 |
| Time to nadir $CD4^+$ T-cells (days) | 15 [9 – 36] | 19 [15 – 28] | 0.122 |
| Set-point# $CD4^+$ T-cells (cells/µL blood) | 602 [257 – 1468] | 154 [80 – 363] | **0.008** |

1066 **Median and range are indicated. p, Mann-Whitney U-test. #Set point defined as Month 3 post-infection**

bioRxiv preprint doi: https://doi.org/10.1101/2019.12.20.885459; this version posted December 21, 2019. The copyright holder for this preprint (which was not certified by peer review) is the author/funder. All rights reserved. No reuse allowed without permission.

# Figure 1

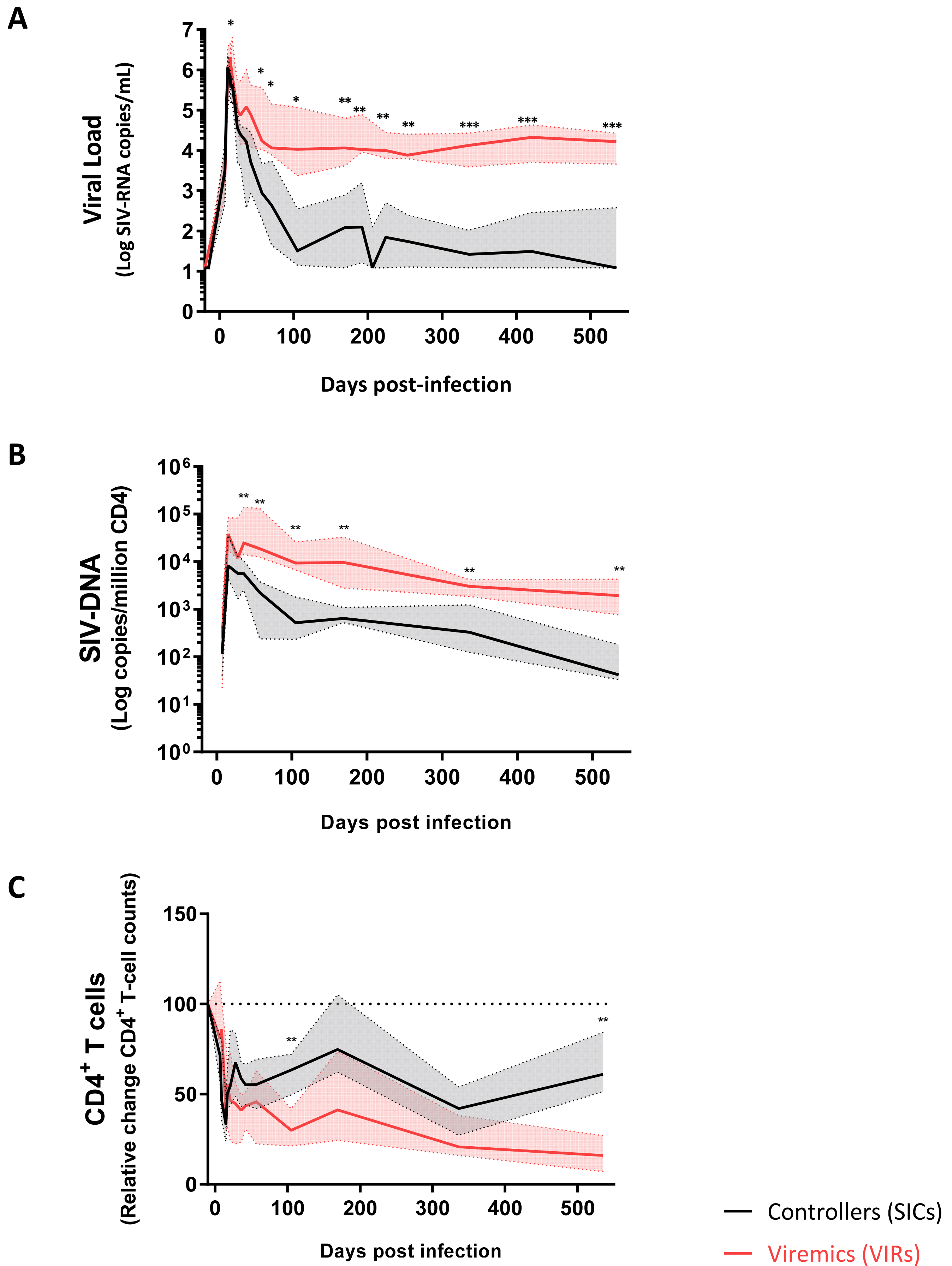

bioRxiv preprint doi: https://doi.org/10.1101/2019.12.20.885459; this version posted December 21, 2019. The copyright holder for this preprint (which was not certified by peer review) is the author/funder. All rights reserved. No reuse allowed without permission.

# Figure 2

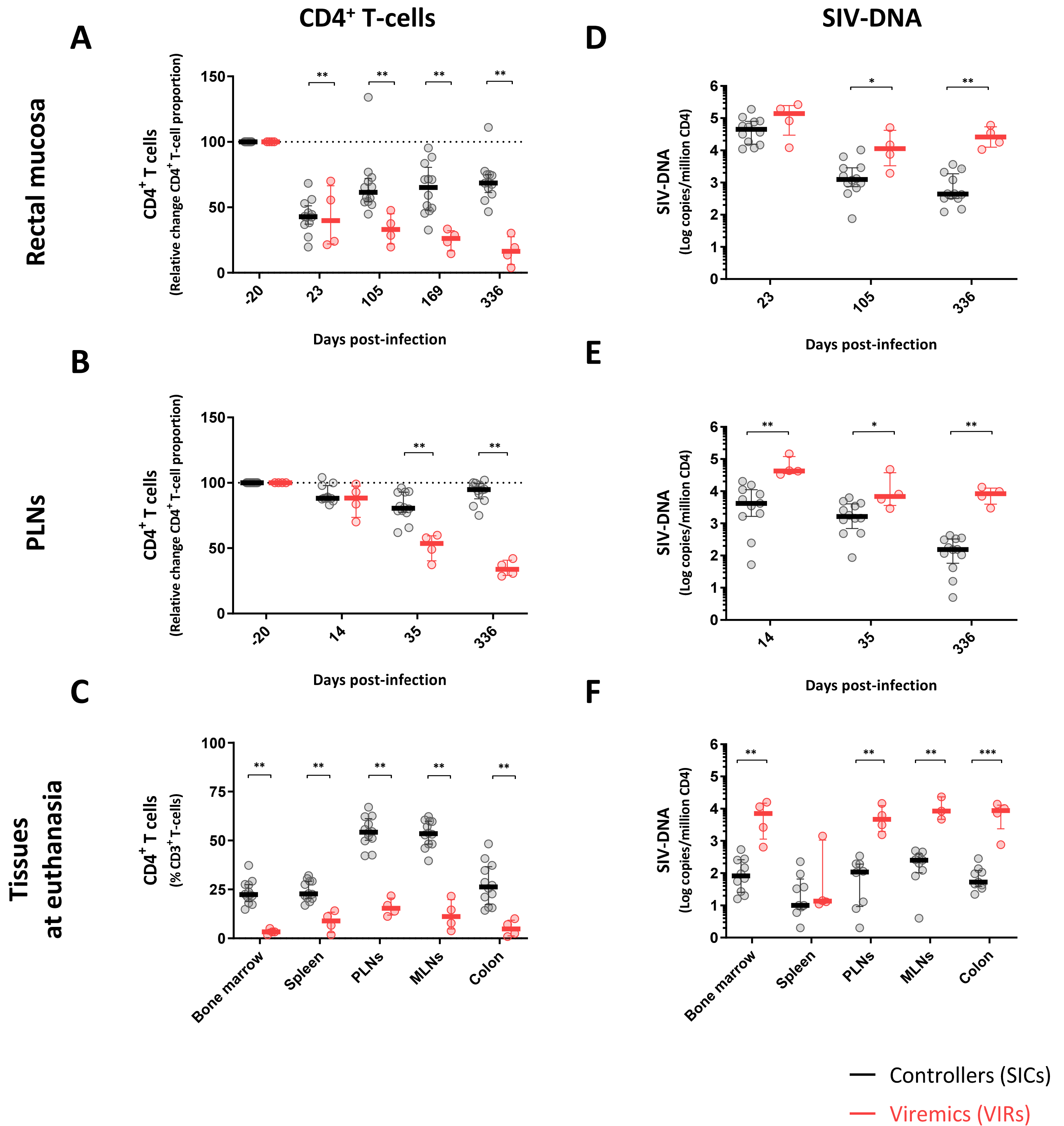

bioRxiv preprint doi: https://doi.org/10.1101/2019.12.20.885459; this version posted December 21, 2019. The copyright holder for this preprint (which was not certified by peer review) is the author/funder. All rights reserved. No reuse allowed without permission.

# Figure 3

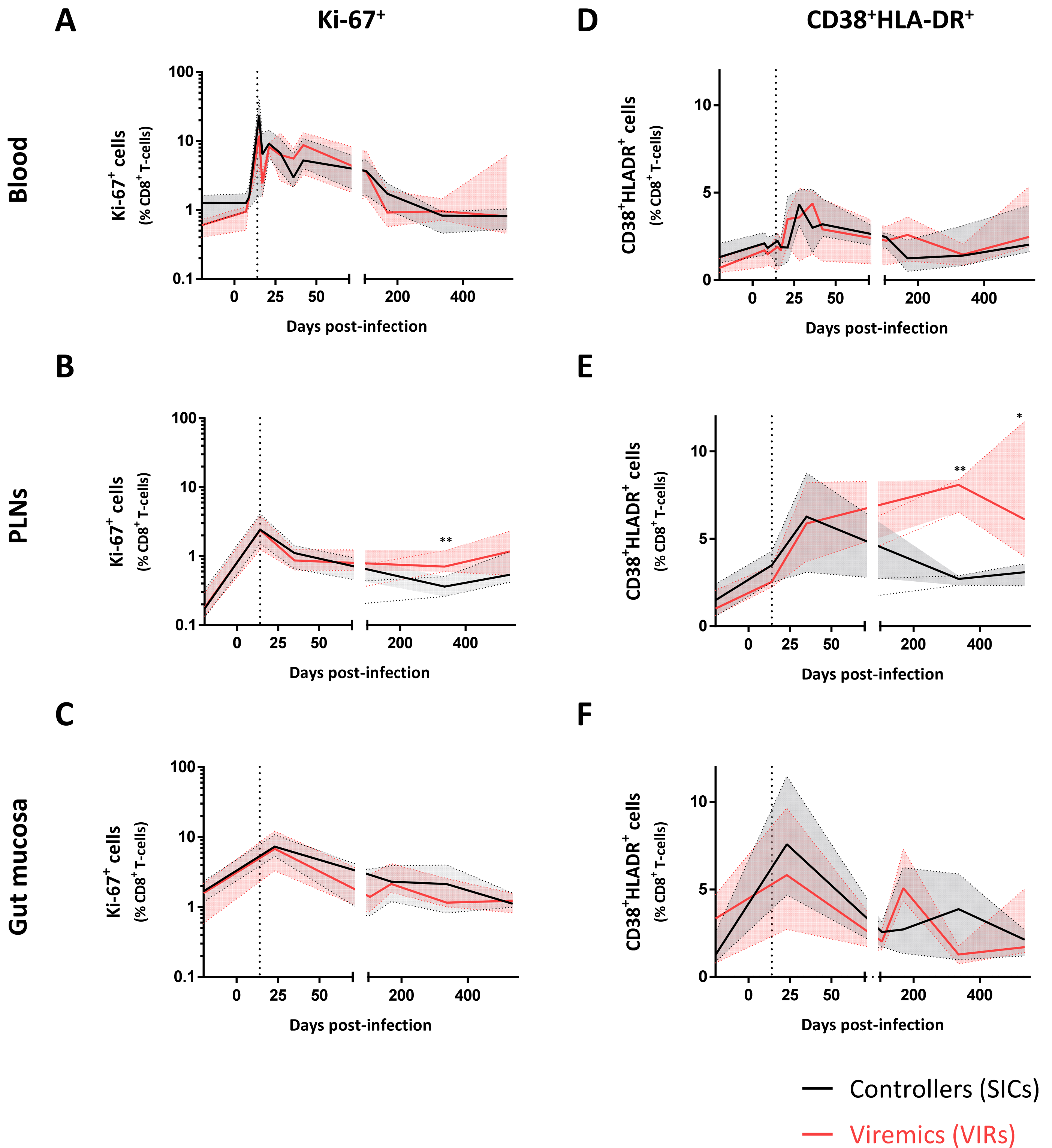

bioRxiv preprint doi: https://doi.org/10.1101/2019.12.20.885459; this version posted December 21, 2019. The copyright holder for this preprint (which was not certified by peer review) is the author/funder. All rights reserved. No reuse allowed without permission.

# Figure 4

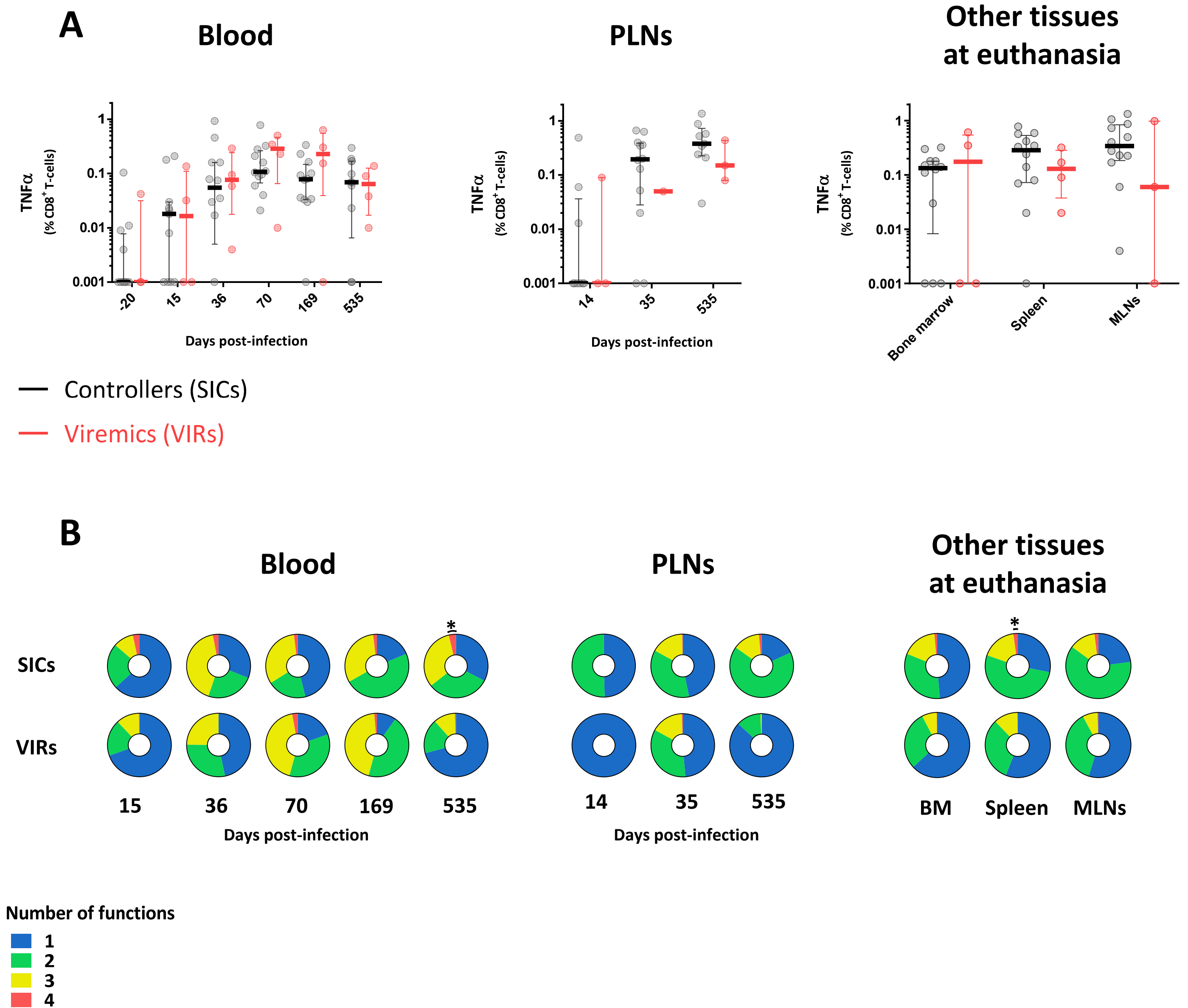

bioRxiv preprint doi: https://doi.org/10.1101/2019.12.20.885459; this version posted December 21, 2019. The copyright holder for this preprint (which was not certified by peer review) is the author/funder. All rights reserved. No reuse allowed without permission.

# Figure 5

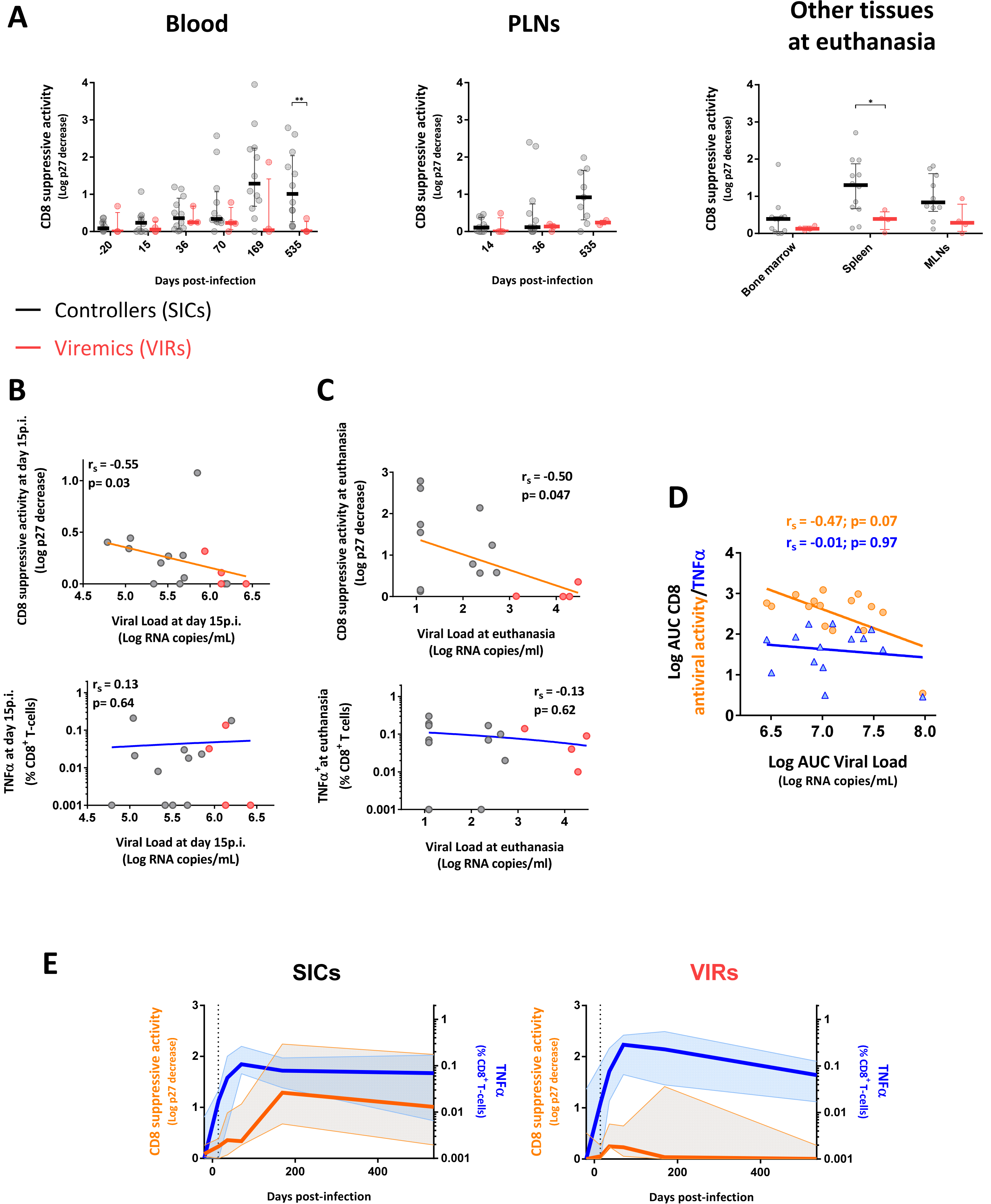

bioRxiv preprint doi: https://doi.org/10.1101/2019.12.20.885459; this version posted December 21, 2019. The copyright holder for this preprint (which was not certified by peer review) is the author/funder. All rights reserved. No reuse allowed without permission.

# Figure 6

## A

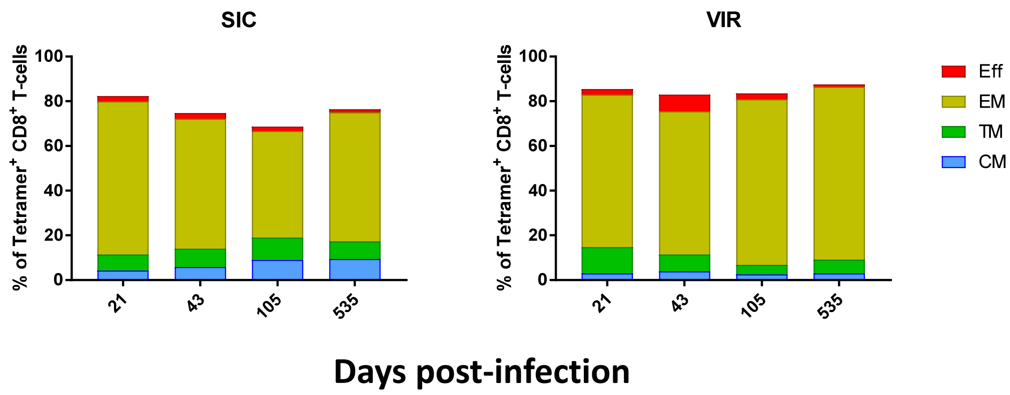


Days post-infection

## B

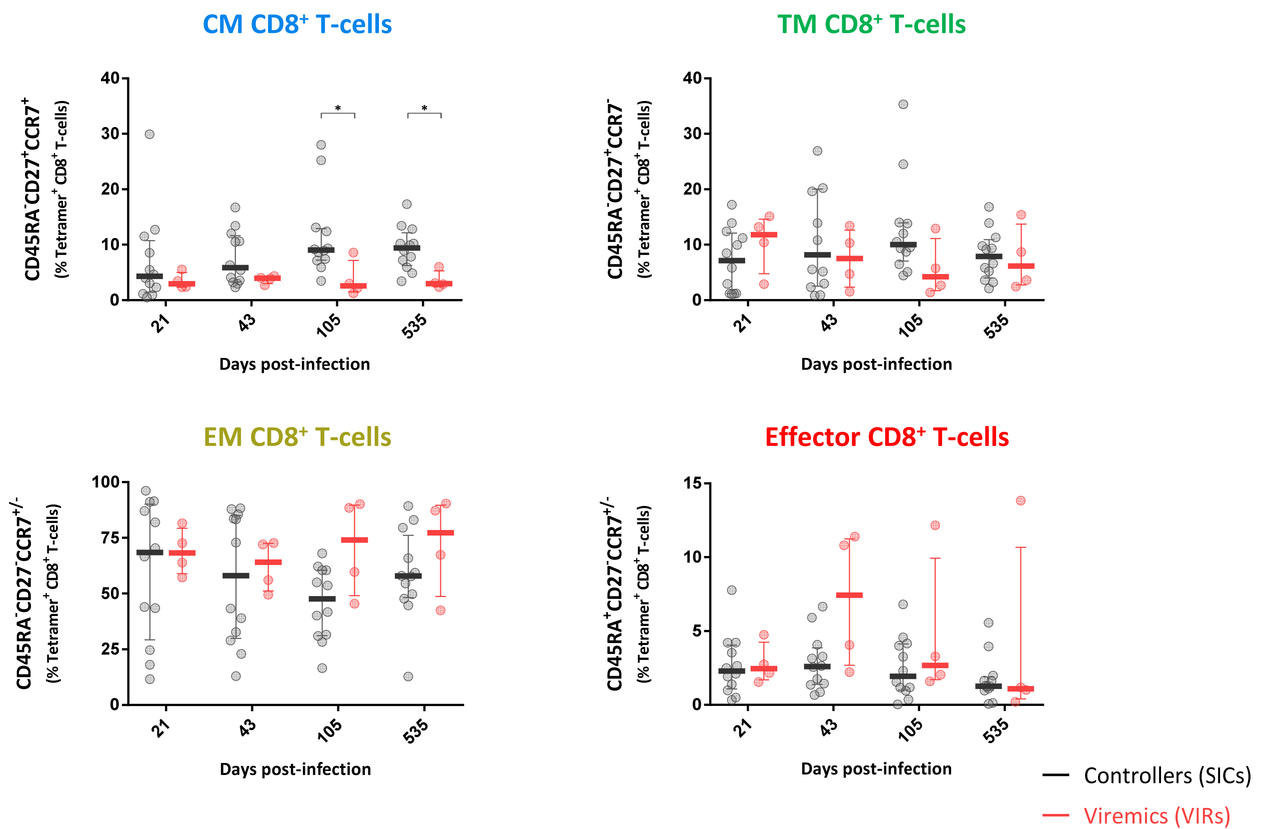

bioRxiv preprint doi: https://doi.org/10.1101/2019.12.20.885459; this version posted December 21, 2019. The copyright holder for this preprint (which was not certified by peer review) is the author/funder. All rights reserved. No reuse allowed without permission.

# Figure 7

## A

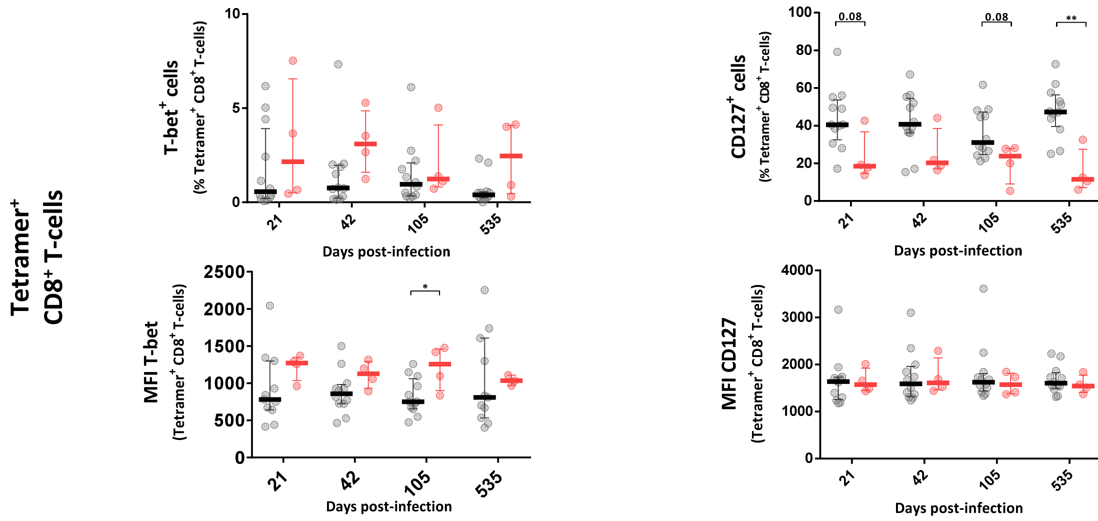


## B

CD8+ T-cell differentiation

Tetramer+ CM CD8+ T-cells

Tetramer+ TM CD8+ T-cells

Tetramer+ EM CD8+ T-cells

Tetramer+ Effector CD8+ T-cells

MFI T-bet (CD45RA-CCR7+CD27+ Tetramer+ CD8+ T-cells)

MFI CD127 (CD45RA-CCR7+CD27+ Tetramer+ CD8+ T-cells)

MFI T-bet (CD45RA-CCR7-CD27+ Tetramer+ CD8+ T-cells)

MFI CD127 (CD45RA-CCR7-CD27+ Tetramer+ CD8+ T-cells)

MFI T-bet (CD45RA-CCR7+/-CD27+ Tetramer+ CD8+ T-cells)

MFI CD127 (CD45RA-CCR7+/-CD27+ Tetramer+ CD8+ T-cells)

MFI T-bet (CD45RA+CCR7+/-CD27+ Tetramer+ CD8+ T-cells)

MFI CD127 (CD45RA+CCR7+/-CD27+ Tetramer+ CD8+ T-cells)

Days post-infection

* 0.06 0.09 0.06 0.08 0.07 0.08 * *

Controllers (SICs)

Viremics (VIRs)

bioRxiv preprint doi: https://doi.org/10.1101/2019.12.20.885459; this version posted December 21, 2019. The copyright holder for this preprint (which was not certified by peer review) is the author/funder. All rights reserved. No reuse allowed without permission.

# Figure 8